Report #1

Submitted on 03 Nov 2016

Referee #1: Stefan Kern, stefan.kern@zmaw.de

Anonymous during peer-review: Yes **No**

Anonymous in acknowledgements of published article: Yes **No**

Recommendation to the Editor

1) Originality (Novelty)
Within the scope of The Cryosphere, does the manuscript represent substantial progress beyond current scientific understanding (new insight, concepts, methods, or data)?
Excellent **Good** Fair Poor

2) Scientific Quality (Rigour)
(A) Is the purpose of the work clearly articulated, reflected in an adequate methodology, and its achievement compellingly underpinned by the evidence presented?
(B) Are the applied methods and techniques valid and suitable?
(C) Are the results discussed in an appropriate and balanced way (consideration of related work, including appropriate references)?
Excellent **Good** Fair Poor

3) Significance (Impact)
Does the manuscript contribute to changing our scientific understanding of a subject substantially or to introducing new practical applications of broad relevance?
Excellent **Good** Fair Poor

4) Presentation Quality
Are the scientific results and conclusions presented in a clear, concise, and well-structured way (number and quality of figures/tables, appropriate use of English language)?
Excellent **Good** Fair Poor

For final publication, the manuscript should be

accepted as is

accepted subject to technical corrections

accepted subject to minor revisions

reconsidered after major revisions

I would like to review the revised paper

I would NOT be willing to review the revised paper

rejected

Please note that this rating only refers to this version of the manuscript!

We thank you once again for your comprehensive report on our revised submission. You point out some important issues, all of which we will address in the following.
Please refer to the new revised version of the manuscript for all applied changes and/or corrections.

Suggestions for revision or reasons for rejection (will be published if the paper is accepted for final publication)

Review of

Circumpolar polynya regions and ice production in the Arctic: Results from MODIS thermal infrared imagery for 2002/2003 to 2014/2015 with a regional focus on the Laptev Sea - Revision 01

by
Preußer, A., et al.

I thank the author team for their careful consideration of the reviewer's comments and concerns. Reading the rebuttal letter doesn't leave anything open except one thing:
I wrote: Page 6, Line 14/15: I understand that the authors mention March here as this month contains the spring equinox. However, November is almost as close to the winter solstice as February is. Could it be that in November the cloud coverage is the problem?
You replied: Including the months of October and April would be problematic since the amount of suitable clearsky and nighttime MODIS scenes decreases with increasing amounts of solar radiation.
My comment (again): In the 1st version of the manuscript you wrote:
Because of the restriction to nighttime scenes, a less frequent IST coverage is present in the beginning (November) and at the end (March) of each winter-season.
Winter solstice is on December 21, right? Therefore sun elevations and hence day lengths are similar on November 21 and January 21, on October 21 and February 21, and so on. From that I'd expect that the number of nighttime cases is similar for the month pairs December/January, November/February, and October/March. Therefore I felt that mentioning November and March in one sentence explaining the limitation to fewer valid cases does not fit and was suggesting in my former review that clouds might have had a larger impact in November - which is something found in the literature as well.
We apologize for not being precise enough in our previous reply, as you are right about this irritating formulation. What we had in mind was the decreasing amount of available MODIS swaths before (so also November) and after the winter solstice, but of course especially March suffers from the increasing amount of shortwave radiation. This is exemplary illustrated in the Fig. below, which shows the daily amount of MODIS swaths (north of 68°N) with valid IST information in 2013/2014. Overall, we don't see a significantly increased effect of clouds in November.

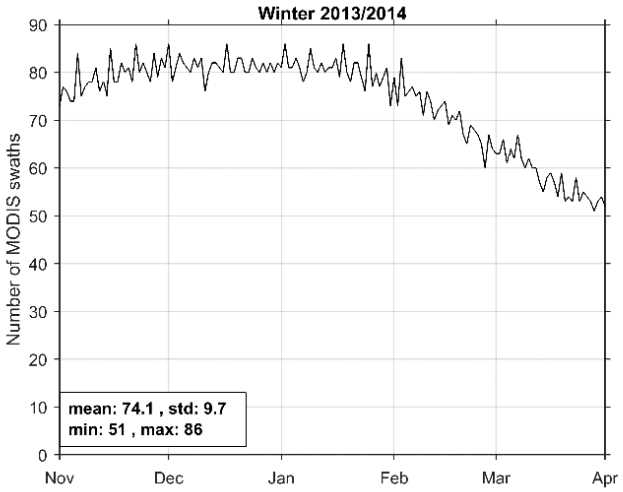

We rephrased this part to make it more concise. It now reads:
"(…) Because of the restriction to nighttime scenes, a less frequent MODIS coverage is present especially towards the end (February to March) of each winter-season."

##################################

General comment:

The manuscript has improved substantially and is almost ready to go.

However, I still have a concern about the usage of polynya area and the associated ice production. The fact that previous studies used similar regions as are used in this study should not prevent the authors from pointing out potential shortcomings of those definitions.
- I strongly suggest therefore that the authors clarify their understanding of a polynya (in the context of how WMO defines it) and their usage of polynya area.
- I suggest further that the authors think one more time about the way they include the results of regions WNZ and KAR into their analysis and results and state even more clearly that their results of particularly these two regions are heavily influenced by ice formation in a MIZ rather than in a polynya.

We understand that especially at the beginning of a winter season, text-book / WMO definitions of a polynya might not be fulfilled in every polynya (i.e. thin ice) region, first and foremost those in the Atlantic sector of the MIZ as you correctly mention (KAR, WNZ, SVA). [*However, this somewhat more frequently appearing "MIZ behaviour" evolved gradually over the investigated period and became more common just in the last 4-5 winter seasons.*]

In the revised MS, we already mention the MIZ influence for the indicated regions (from which the WNZ was specifically requested by Referee #3), but we could highlight this more clearly as you correctly point out.

Although we share some concerns regarding MIZ characteristics, we nevertheless decided to include the WNZ region to ensure comparability to earlier studies. To quote our response to Referee #3:
"In recent years, the area at the northern tip and western coast of Novaya Zemlya was rarely fully enclosed by sea ice during winter. Initially, this was one of the main reasons why we decided to exclude this region as seemed to more fulfill MIZ characteristics in our opinion. Nevertheless, motivated by the reviewers comment we took a closer look at this region and decided to include it in an updated / revised version of the manuscript. Following Årthun et al. (2012), at the least the influence of the eastern branch of Atlantic water spreading into the Barents Sea seems to be lower as expected in this region. ***It remains up for debate if those regions with changing ice conditions in recent years can be considered as a polynya region in a textbook sense, but in order to increase consistency regarding the considered polynya regions to Tamura and Ohshima (2011) and Iwamoto et al. (2014) the manuscript was changed accordingly with an additional polynya mask "Western Novaya Zemlya" (WNZ).*** *Necessary changes can be found to the marked up version of the manuscript."*

Further down, you highlight this year's unusually late freeze-up as an example of large-scale freeze up conditions. We expect that this development will continue to extend further into Nov./Dec. over the next years/decades which will eventually lead to some necessary adaptions in our approach for future investigations.

To address this topic in the MS, we now added the following part to Sect. 1:

"The marginal ice zone (MIZ) in Fram Strait and northern Barents Sea is mostly excluded in our investigations due to a variety of potential ambiguities originating from ocean heat fluxes and a high interannual variability of the MIZ in terms of location and extent. However, in order to ensure consistency to previous studies, the MIZ is to some extent included in the CHU, STO, NOW, WNZ and KAR areas. For those regions, this implies that the here derived characteristics may contain periods with extensive ice-free conditions, first and foremost in early winter."

And the following part to Sect. 3.3:

"The complete period from November to March each winter is considered for the calculation of POLA / IP, which implies that the here derived values are potentially influenced by shifts in the timing of freeze onset during the early freezing season (November / December). **For potentially MIZ-influenced regions (CHU, SVA, NOW, WNZ, KAR), this has to be considered when comparing metrics derived for the full winter period (November to March).**"

These two concerns plus the specific comments led me to the suggestion that the authors should have the chance to for a minor revision which are to the authors' discretion, i.e., there is no need for me to have another review.

Specific comments / suggestions / typos:

P4, L31: Please check meaning of "inhibit". I would go for "contain" or "exhibit".
Replaced by "contains".

P5, Figure 2, Caption, 3rd line: "'IST' denotes to …" Please either change "to" to "the" or omit completely.
Fixed.

P6, Lines 6-12: I suggest to add the information that the approach assumes a sheet of ice being present, i.e. that is not able to include the frazil / grease ice stadium.
Slightly changed to: "(…) the approach does not explicitly discriminate between different ice types within a polynya, as TIT are solely derived from calculating the heat conduction in/through **an assumed layer of ice** (aside from subsequent gap-filling; see Sect.~3.2)."

P6, Line 23: The authors could motivate the usage of the median instead of the mean in one additional sentence.
It now additionally reads: "The median is preferred over a simple average in order to reduce the potential risk of erroneously high or low values in single swaths, originating e.g. from unidentified clouds."

P6, Line 31: "completely uncovered pixels" means that there are no MODIS data available?
This is exactly the case.

P8, Line 16: "weighted average" Does this averaging use the same weights as mentioned above in Lines 11-12?
You are right, the same weights are used. We added this to L.16.

P8, Line 26: Please define "POLA".
As "POLA" is introduced a bit later in Sect. 3.3, the part here is slightly altered to read "(…) yielded superior results both in spatial correlation and **reconstructed polynya extent**, regardless of (…)"

P10, L9: How is Q_ice computed? I assume it is computed per pixel and it is computed as a function of the daily composite TIT of that respective pixel? I guess an additional sentence clarifying the procedure would help.
The conductive heat flux through the ice (Q_ice) and with that the equal atmospheric heat flux Q_atm is indeed calculated pixel-wise. Q_ice is defined as

$$Q_{\mathrm{ice}} = \kappa_{\mathrm{ice}} \times \frac{(T_{\mathrm{surf}} - T_{\mathrm{f}})}{h_{\mathrm{ice}}} \quad \text{(Eq.1)}$$

To quote Preußer et al. 2015a (Sect. 2.3):

"To obtain the ice thickness (h_ice), the total atmospheric flux Q_atm (Eq. 2) is set equal to the conductive heat flux through the ice (Q_ice; Eq. 1), and Eq. (1) is solved for h_ice using a value for the thermal conductivity of κ_ice = 2.03 Wm^–2 K^–1 (Drucker et al., 2003)."
However, we do not think it is necessary to include this once again, as the reader is already referred to the indicated references for further details on the (well-known) procedure (Yu and Rothrock (1996), Yu and Lindsay (2003), Drucker et al. (2003), Willmes et al. (2010/2011), Adams et al. (2013), Preußer et al. (2015a,b), Paul et al. (2015b), etc.).

P10, L24: "areal extent of each pixel" Would it be fair to assume that this is 4 km²?
This is correct, the average extent of a pixel is around 4 km². However, due to the currently used equirectengular grid the resolution in longitudinal direction is slightly varying with latitude, so that it increases south and decreases north of 79°N.

P10, L25: "extrapolated to daily rates" One could also write instead: "multiplied by 86400 to obtain IP / day."
Despite this reasonable remark, we decided to keep the current formulation at this point of the MS.

P11, Line 3: "stable cloud cover": In line 5 you write "persistent" instead of stable. I suggest to use "persistent" throughout.
Fixed accordingly, thank you.

P11, Lines 6-9 + Figure 4: While these 3 lines are a step into the correct direction I would suggest to take into account two more important aspects here:
i) Starting early in the freezing season might imply that the definition of a polynya is simply not yet fulfilled. Hence what is termed "POLA" is not POLA because it is not related to a polynya by definition. A look at Figure 4, November, reveals this clearly: In the eastern Kara Sea TIT frequencies are low because the thick ice has arrived. Polynyas at Islands and along the coast can be delineated. Towards the southwest TIT frequency first increases and then decreases again towards the Kara Strait. The fact that TIT frequency is low close to the Kara gate is due to the fact that sea ice is still absent there (on average) in November and that the Kara Strait is presumably still open. Kern et al. (2005, Geophys. Res. Lett.) stated:
"*In each season the PSSM (e.g. polynya area retrieval) analysis starts once the entire Kara Sea is ice covered or an ice bridge has formed in the Kara Strait so that the remaining open water area inside the Kara Sea can be regarded as a polynya. The such defined starting date varies from mid-November to the end of December.*"
Because of this the results of Kern et al. (2005) and Kern (2008) are based on the period January to April – to ensure that what is targeted in the conclusions and interpretations is in fact associated with a polynya.
Please note also that the results of Kern (2008) are based on coarse resolution (25 km and 12.5 km, Backus-Gilbert interpolated to 12.5 km and 5 km) SSM/I data with the respective limitations detailed already by the authors.
ii) The same applies to the IP. If one would choose 2016 (we are at the beginning of November right now) more or less the entire Kara Sea is still ice free. The same would apply (currently) to regions WNZ, STO, BSH, CHU, half of ESS, and NOW. The entire ice production happening in the Kara Sea would be included into an estimate of the ice production which according to your paper is associated with ice production in a polynya. What one would in fact include is open ocean ice production. Yes, I agree that the advance of the ice-edge can be rather quick and the time between still open water and a closed sea ice cover of thickness > 0.2 m can be a few days only and the associated IP will be like noise. I tend to say though that freeze-up of region KAR and WNZ takes longer.
One would also assume that the entire ice production in these still large open water areas is due to thermodynamics. This is certainly a fair assumption for TIT < 0.2 m. However, one cannot consider effects such as rafting (due to wind but also due to tidal forcing) and one cannot consider the fact

that a substantial part of the sea ice might be of type pancake ice which has a substantial dynamic formation component.
I guess the same **applies to region WNZ where particularly the southern part might not be ice covered at all during November through March** (at least when I browse through sea-ice concentration maps of the period 2002/03 through 2014/15 I'd say that in half of the winters region WNZ was ice free most of the time). For the region SVA only the south-eastern part is influenced by MIZ activities. The Whaler's Bay polynya north of Svalbard, which is known as a sensible heat polynya is included into region SVA, however.

I suggest to, in the context of Figure 4 and its interpretation, **A) describe how the TIT frequency is computed** (does this include open water cases?) and **B) stress that areas with low TIT frequency can be both sea ice or open water**.
I am asking for A) because I am quite surprised to see the fracture event occurred in Feb 2013 in the Beaufort Sea (see Beitsch et al., 2014) to pop up in the TIT frequency map of FEB while the fact that large parts of the Kara Sea where essentially ice free in February 2013 seems not to have added to the TIT frequency. Therefore I am curious to learn from which measure the TIT frequency is computed (all native clear-sky IST cases – or all cases where a TIT value is present no matter whether it is native or interpolated) and what is the basis to make it a relative measure.
Thanks for this extensive remark which will hopefully help to clarify some potential interpretation-difficulties.

Regarding the computation of TIT frequencies (Remark A+B) in Fig.4, the presented numbers are the relative appearance rate, **i.e. the fraction of TIT≤ 0.2m detections per pixel (based on daily composites; including interpolated TIT), relative to the total amount of days between 2002/2003 and 2014/2015** (example for one polynya-pixel in January: e.g. 150 thin-ice detections in total in a maximum period of 13winters*31days (=403) days → TIT frequency = 0.37).
The thickness range of TIT≤ 0.2m theoretically includes all TIT between 0 and 20 cm, but due to the circumstance that a TIT of exactly 0cm is only possible in theory using the calculation with Q_ice (the IST would have to be exactly equal to Tf = 271.35K), open water in the sense of TIT=0cm is if at all only rarely included in our results. However, very thin ice (0cm < TIT < ~1-2cm) is frequently calculated.
Concerning your specific example for the Kara Sea in February (did you mean 2012?), (prolonged) ice-free conditions imply that there is potentially no IST available (temperature above freezing) at those locations and consequently – no TIT. But, as you correctly remark, thin ice can appear under those circumstances as kind of a noisy pattern for pixels where IST and hence TIT are available.
In case of the lead-event in the Beaufort Sea, we assume that thin ice in this broad, enduring and extensive area was correctly detected by our algorithm and is therefore also visible in Fig.4.

We added the following sentence when introducing Fig.4:
"**Monthly thin-ice frequencies, calculated per pixel as the fraction of days with a TIT $\leq$ 0.2\unit{m} relative to the 13-yr investigation period, are presented in Fig.~4.**"

In addition, the caption of Fig.4 is slightly modified to read:
"Average wintertime (November to March) frequencies of TIT ≤ 0.2 m in the Arctic between winters 2002/2003 and 2014/2015. **For each month, frequencies are calculated per pixel as the fraction of days with a TIT $\leq$ 0.2\unit{m} relative to the 13-yr investigation period.** (…)"

P11, Lines 21/22: Please stress that the average TIT is computed only from pixels with TIT < 0.2 m and not from the fraction (COV4) of the open ocean area. This is important to avoid misinterpretation of your results. Perhaps you could put the TIT values into a separate table together with the POLA?

It seems likely to us that you might still be a bit confused by the "COV4" numbers. As we wrote in our first response letter, this measure refers to the **spatial coverage of MODIS data**, i.e. the availability of valid (clear-sky, HQ MCP, SFR) IST/TIT value-pairs inside a respective polynya mask area. Hence, it is not a fraction of open ocean area.
You are right however, that these average TIT values are calculated only for TIT ≤ 0.2m. We indicated that both in the caption of Tab.1 and in the MS (Sect. 4.1: "*Interannual average values for TIT ≤ 0.2 m are listed in Tab. 1 for each polynya region.*") and think that this should be sufficient, considering that this thickness-range is the basis of all results presented throughout the MS. Regarding the remark on a separate additional table, we would also sincerely dismiss this suggestion, as this basic information fits well into the context of more or less general information on each region.

Page 13, Line 8: Please check usage of "compliment". Perhaps "complement" would fit better?
It sure fits better, compliment to you for this suggestion/remark.

Page 13, Line 10: "this" → "these"
Fixed, thank you.

Page 16, Line 11 to Page 17, Line 9: I am glad the authors do mention here the fact that freeze-up has an impact on both POLA and IP particularly during Nov./Dec. To my opinion it is not only the freeze-up which has an impact but also the fact that some of the regions simply remain ice free has an impact. I'd tend to say that the decreasing trend of IP in region WNZ, for example, is simply a cause of a general decrease of the sea-ice cover in that region. In Line 6 on page 17, I suggest to refer to region SVA instead of region Storfjorden polynya.
Regarding the open-water influence, we supplemented the respective part accordingly. However, the Storfjorden / Svalbard area is now removed in that context, as (a) the seasonal contrast is more pronounced in the other named regions and (b) it shortens this exemplary list, thereby enhancing the reading flow in our opinion.
It now reads: "In case of e.g. the Kara Sea, Franz-Josef-Land, the Chukchi Sea and the Canadian Arctic Archipelago**, large thin-ice and potential open-water areas** during the early freezing period in November and December (…)"

Page 17, Line 7: The fact that region NOW stands out that much is again caused by a substantial fraction of IP during freeze-up. This is indicated partly by the high IP values in the fjords which become covered with fast ice in December/January (see Preusser et al., 2015, Remote Sensing, 7).
This effect certainly contributes to the observed distribution of high IP areas.

Page 19, line 11/12: Instead of "the net effect … here" the authors could write: "would require a theoretical study where an artificial polynya is investigated using several different spatial resolutions." As this would point towards a future direction of research.
Despite this good suggestion, we decided to keep the current formulation at this point of the MS.

Page 20, Lines 3-4 versus Line 7: I find that the notions of "suggests a southward shift of the fast-ice edge" and "shape and location of the fast-ice edge did not vary significantly" contradict each other and could lead to a misunderstanding. Perhaps the authors could reformulate this part. A suggestion would be: "… and (2) we observe opposing negative / positive IP-trends along the coasts of the Laptev and Kara Seas which could be due to changes in fast-ice extent. Decreasing …"
We modified the respective part as suggested to read:
"(…) and (2) we observe opposing negative / positive IP-trends along the coasts of the Laptev and Kara Seas which could be due to changes in fast-ice extent over the 13-year period."

Page 20, Lines 11-17: This is a quite global statement which could be strengthened. I suggest *to i) refer to when in particular 2m-air temperatures have been increasing (which season?), to ii) stress*

that delayed freeze-up and longer open water seasons may easily lead to increased POLA and IP which could counterbalance smaller IP caused by warmer air temperatures, and to iii) *be more specific how and why a downward trend in sea-ice volume can have an influence on POLA and IP.*
A downward trend in sea-ice volume (and hence ice thickness) would theoretically result in a more fragile and more mobile sea ice cover in the Arctic with an increased sensitivity for external forcing mechanisms responsible for thin ice / polynya-openings (e.g. wind, ocean currents). However, this part of the manuscript was meant to highlight the processes and factors that contribute or interact to/with a shortening of the freezing season at high latitudes, thereby indirectly influencing POLA and IP though longer open-ocean periods. One of the recent studies on year-round increasing temperatures (~Arctic Amplification) in most regions of the Arctic was recently published e.g. by Cohen et al. (2014)[1].

We modified the part at the end of Sect.4.1 to now read:

"(…) could be connected to an overall later appearing fall freeze-up (Markus et al., 2009; Stroeve et al., 2014) in recent years, which itself is thought to result from a complex mixture/interplay of steadily and **year-round** increasing (2m-) air temperatures (**e.g. Cohen et al., 2014**), distinct large-scale atmospheric patterns (e.g. Rigor et al., 2002) and the overall downward trend of total sea-ice extent and volume in the Arctic (e.g. **Schweiger et al., 2011; Laxon et al., 2013**). **The latter implies a tendency towards a more fragile, thus mobile, sea-ice cover in the Arctic, with a potentially increased sensitivity for external forcing mechanisms (i.e. strong winds and/or ocean currents) that are responsible for thin-ice formation in polynyas and leads.**"

In addition, due to similar explanations, we had to slightly reformulate a short part in Sect.4.2, which now reads:

"For the period from 1982 to 2009, the study by Kwok et al. (2013) presented indicators for a net-strengthening of both the Transpolar Drift and the Beaufort Gyre as well as a general increase of the Arctic ice drift-speed**, which is presumably related to a decreasing fraction of thick multi-year (MY) ice. As mentioned before (Sect. 4.1), the latter is thought to be connected to an increased fragility and mobility of the Arctic sea-ice cover, which may have implications for polynya and lead dynamics not only in the eastern Arctic.**"

Page 22, Line 11: "it has to noted" → "it has to be noted"

Fixed, thank you.

Page 24, Figure 12: The annotation in the upper left corner of the image and the y-axis annotation says: "Ice Export Area" while the caption speaks of "Ice Area Export". Which is correct?
"Ice Area Export". We fixed **Fig.12** accordingly.

Page 26, bullet (1): You could add that with this spatial resolution you can go much closer to the coast and land spill over effects are efficiently mitigated.
Bullet (2): Given the concerns formulated above I suggest the authors stress that the IP mentioned here is not necessarily from ice production in a polynya but includes open ocean ice production. Further in this bullet you could formulate more concisely instead of "Compared to …": "Our estimate of the average total ice production exceeds that of Iwamoto et al. (2014) by about 50%. We note that differences … „

[1] Cohen, J., Screen, J. A., Furtado, J. C., Barlow, M., Whittleston, D., Coumou, D., Francis, J., Dethloff, K., Entekhabi, D., Overland, J., Jones, J. (2014): Recent Arctic amplification and extreme mid-latitude weather. *Nature geoscience*, *7*(9), 627-637.

We modified the respective part to read:

"(1) The use of high-resolution MODIS data enables the detection of thin ice much closer to the coast or fast-ice edges, mitigates land spill-over effects efficiently and generally increases the capability to resolve small scale (> 2km) thin-ice features such as narrow polynyas and leads, which therefore contribute to our ice production estimates. This represents an advantage compared to other (passive microwave) data sets.

(2) The average wintertime accumulated ice production in all 17 polynya regions is estimated with about 1811 ± 293 km³. The largest contributions originate from the western proximity of Novaya Zemlya (20%), the Kara Sea region and the North Water polynya (both 15%) as well as scattered smaller polynyas in the (eastern) Canadian Arctic Archipelago (all combined around 12%). By relying on predefined and fixed polynya masks, these IP estimates can include both thermodynamic ice growth within detected polynya margins (TIT ≤ 0.2 m) as well as ice production in open ocean / MIZ areas. However, our estimate on the average total ice production exceeds that of Iwamoto et al. (2014) by about 52-54%. We note that differences in the regarded time frame, reference areas, sensor-specifics as well as a potential bias due to cloud cover and/or the exclusive assumption of clear-sky conditions certainly contribute to this discrepancy."

Circumpolar polynya regions and ice production in the Arctic: Results from MODIS thermal infrared imagery for 2002/2003 to 2014/2015 with a regional focus on the Laptev Sea

Andreas Preußer[1], Günther Heinemann[1], Sascha Willmes[1], and Stephan Paul[2]

[1]Department of Environmental Meteorology, Fac. of Regional and Environmental Sciences, University of Trier, Behringstr. 21, Trier, D-54296, Germany.
[2]Alfred Wegener Institute, Helmholtz Centre for Polar and Marine Research, Am Handelshafen 12, 27570 Bremerhaven, Germany.

Correspondence to: Andreas Preußer (preusser@uni-trier.de)

Abstract. High-resolution MODIS thermal infrared satellite data are used to infer spatial and temporal characteristics of 17 prominent coastal polynya regions over the entire Arctic basin. Thin-ice thickness distributions (≤ 20 cm) are calculated from MODIS ice-surface temperatures, combined with ECMWF ERA-Interim atmospheric reanalysis data in an energy balance model for 13 winter-seasons (2002/2003 to 2014/2015; November to March). From all available MODIS swath-data, (quasi-) daily thin-ice thickness composites are computed in order to derive quantities such as polynya area and total thermodynamic (i.e. potential) ice production. A gap-filling approach is applied to account for cloud and data gaps in the MODIS composites. All polynya regions combined cover an average thin-ice area of 226.6 $\pm$ 36.1 $\mathrm{x10^3 km^2}$ in winter. This allows for an average total wintertime accumulated ice production of about 1811 $\pm$ 293 $\mathrm{km^3}$, whereby the Kara Sea region and the North Water polynya (both 15%), polynyas at the western side of Novaya Zemlya (20%) as well as scattered smaller polynyas in the Canadian Arctic Archipelago (all combined 12%) are the main contributors. Other well-known sites of polynya formation (Laptev Sea, Chukchi Sea) show smaller contributions and range between 2 and 5%. We notice distinct differences to earlier studies on pan-Arctic polynya characteristics, originating to some part from the use of high-resolution MODIS data, as the capability to resolve small scale (> 2km) polynyas and also large leads is increased. Despite the short record of 13 winter-seasons, positive trends in ice production are detected for several regions of the eastern Arctic (most significant in the Laptev Sea region with an increase of 6.8 $\mathrm{km^3}$/yr) and the North Water polynya, while other polynyas in the western Arctic show a more pronounced variability with varying trends. We emphasize the role of the Laptev Sea polynyas as being a major influence on Transpolar Drift characteristics through a distinct relation between increasing ice production and ice area export. Overall, our study presents a spatially highly accurate characterization of circumpolar polynya dynamics and ice production which should be valuable for future modeling efforts on atmosphere- sea ice - ocean interactions in the Arctic.

1 Introduction

The sea ice cover in the Arctic is subject to continuous changes through a variety of thermodynamic and dynamic processes, which are driven by atmosphere and ocean dynamics. Areas of open water and thin ice, i.e. polynyas and leads, are characteristic

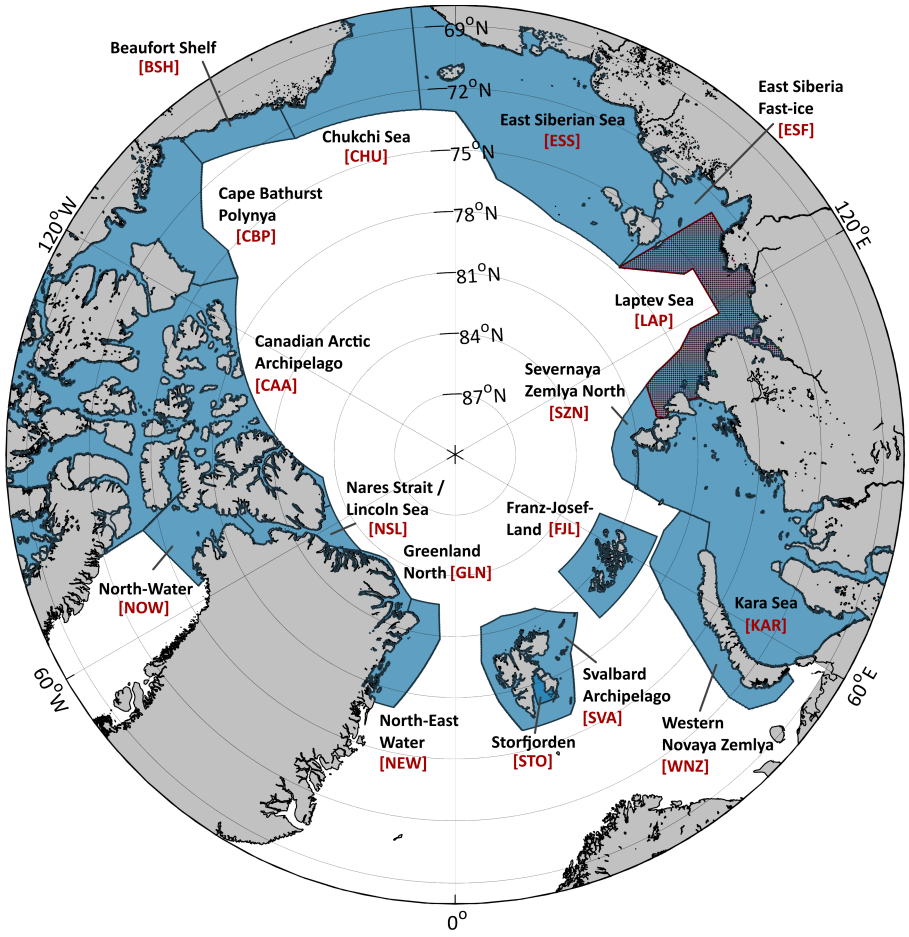

Figure 1. Map of all investigated areas of interest located in the Arctic, north of 68° N. Except for the Laptev Sea (red frame), all other applied polynya masks are marked in blue and enclose the typical location of each polynya in wintertime.

features in this ice scape with a huge influence on local physical, biological and chemical processes at the interface between the atmosphere and the ocean (Barber and Massom, 2007).

Especially during wintertime, the presence of open water and thin ice leads to increased ocean to atmosphere heat fluxes, thereby allowing for new ice production and brine release as well as generally strong modifications of both the atmospheric boundary layer and upper ocean layers (Ebner et al., 2011; Gutjahr et al., 2016). Hence, an accurate assessment of wintertime sea-ice production in the Arctic is of vital interest for the understanding of Arctic sea-ice dynamics, the annual sea ice mass balance and, in general, for the verification of climate and ocean models. In case of the Arctic, it is widely considered that the main mechanism for polynya and lead openings are divergent ice motions caused by wind-induced stress (Smith et al., 1990). Therefore, most Arctic polynyas can be found adjacent to or in proximity of a fixed obstacle such as the coastline, attached land-fast ice or ice bridges under offshore-wind conditions (Williams et al., 2007). While the time of formation, the duration

and the spatial extent of a polynya can be highly variable from year to year, their location of formation is generally rather stable (Morales-Maqueda et al., 2004). Leads are, in contrast, by far more variable both in space and time (Willmes and Heinemann, 2016). A regular monitoring of these open water and thin-ice areas with a high spatial accuracy is therefore a crucial step to be able to detect long-term changes, potential linkages and feedbacks to other environmental compartments as well as spatial and temporal patterns.

Based on the inventory of Barber and Massom (2007), we here define a total of 17 individual polynya regions in the Arctic north of 68° N (Fig.1). Some of these areas are designed to match reference areas in previous studies (e.g. Kern, 2008). The areal extent, i.e. the total ocean area, of each sub-region is depicted in Tab. 1. The vast majority of polynyas of our study is located around the Arctic shelf areas, with the largest fraction in the Siberian shelf region (East Siberian Sea (ESS), Laptev Sea (LAP), Severnaya Zemlya North (SZN), Kara Sea (KAR), Western Novaya Zemlya (WNZ)). Other well-known sites of polynya formation are the North Water (NOW) Polynya in northern Baffin Bay, several other frequently appearing thin-ice zones around northern Greenland (Nares Strait / Lincoln Sea (NSL), Greenland North (GLN), North-East Water (NEW) polynya), the Storfjorden (STO) polynya in the Svalbard Archipelago (SVA) and a number of smaller polynya locations around Franz-Josef Land (FJL), the Canadian Arctic Archipelago (CAA) as well as the Beaufort (BSH and CBP) and Chukchi (CHU) Seas. The marginal ice zone (MIZ) in Fram Strait and northern Barents Sea is mostly excluded in our investigations due to a variety of potential ambiguities originating from ocean heat fluxes and a high interannual variability of the MIZ in terms of location and extent. However, in order to ensure consistency to previous studies, the MIZ is to some extent included in the CHU, STO, NOW, WNZ and KAR areas. For those regions, this implies that the here derived characteristics may contain periods with extensive ice-free conditions, first and foremost in early winter.

Pan-Arctic estimations of daily thin-ice thicknesses and ice production in polynyas were previously published by Tamura and Ohshima (2011) and Iwamoto et al. (2014), who both presented newly developed empirical thin-ice algorithms. Therein, commonly used passive microwave remote sensing data from the Special Sensor Microwave / Imager (SSM/I) and Advanced Microwave Scanning Radiometer - EOS (AMSR-E) satellite sensors is related to reference thin-ice thicknesses from Advanced Very High Resolution Radiometer (AVHRR) and Moderate Resolution Imaging Spectroradiometer (MODIS) thermal infrared data, based on a characteristic inverse relationship between the surface brine volume fraction and the thickness of sea ice (Iwamoto et al., 2014). In both studies, the advantages of passive microwave systems (complete daily coverage in the Arctic, almost no influence of clouds) come at the cost of quite coarse spatial resolutions (6.25 - 25 km) which strongly limit the ability to resolve small and/or narrow thin-ice areas in close proximity to coastlines or along fast-ice edges (Preußer et al., 2015a).

According to Willmes et al. (2011), a retrieval of long-term ice production is challenging for several reasons. The derivation of polynya area needs to be addressed with spatial and temporal resolutions that are sufficient to capture the seasonal and regional dynamics of polynya events (Winsor and Björk, 2000; Morales-Maqueda et al., 2004; Tamura et al., 2008; Willmes et al., 2010). Further, the heat loss over the polynya has to be calculated, which requires detailed information about the fraction of open water, the ice thickness and its distribution within the polynya. The distribution of thin-ice largely affects the heat loss by providing feedback on the ice surface temperature, thereby altering the vertical temperature gradients both through the ice as well as towards the lower atmospheric boundary layer. Not less important, an accurate calculation of heat loss requires a

state-of-the-art approach regarding the parametrization of the surface energy balance, turbulent fluxes of latent and sensible heat and the conductive heat flux through the ice. Thus, detailed (i.e. region-specific and ideally highly resolved) information on meteorological quantities and correct formulations for the turbulent exchange coefficient for heat (C_H) are of particular importance (Gutjahr et al., 2016).

In order to address those challenges, the prime focus of this study is aimed towards the derivation of (quasi-) daily spatial thin-ice thickness distributions, which allows for a pan-Arctic retrieval of associated quantities like polynya area and thermodynamic ice production. We make use of a high-resolution and long-term record of thermal-infrared data from MODIS, as measured ice-surface temperatures can be combined with atmospheric reanalysis data in a 1-D energy balance model (Adams et al., 2013) to obtain ice thicknesses up to 50 cm (Sect. 3.1). Based on these daily distributions and taking into account a necessary compensation for inherent cloud- and data gaps (Sect. 3.2), the amount of new sea-ice formation can be determined (Sect. 3.3). In Sect. 4, our achieved results will be presented and discussed, before closing this paper with final conclusions and prospects for further investigations. In recent studies using the same methodology based on MODIS data, we focused on the Storfjorden polynya (Preußer et al., 2015b) and NOW polynya (Preußer et al., 2015a). The present study has a strong focus on the Laptev Sea region due to significant changes over the last decade (Sect. 4.2) as well as its role as a central component of the Transpolar Drift, a large-scale drift system where ice from the Siberian coastal regions is advected across the Arctic Ocean and through Fram Strait.

2 Data

2.1 MODIS ice-surface temperatures

The MOD/MYD29 Collection 5 sea-ice product (Hall et al., 2004; Riggs et al., 2006) is used to derive thin-ice thickness (TIT) from MODIS satellite data. It features swath data of ice-surface temperatures (ISTs) from both MODIS instruments on board the Terra and Aqua polar-orbiting satellite platforms. All swath data offer a spatial resolution of 1x1 km^2 at nadir and include a basic cloud-screening procedure using the MODIS cloud mask (MOD/MYD35; Ackerman et al. (2010)). In general, the accuracy of the MOD/MYD29 ISTs is given with 1–3 K (Hall et al., 2004). All IST swaths covering the Arctic Ocean and adjacent seas were extracted using meta data information for each MODIS swath. Subsequently, single swaths are mapped onto a common equirectangular (reference-) grid covering all areas north of 68° N , with the output resolution set at 2 km in order to account for the decreasing spatial resolution of the MODIS sensor off-nadir. For our analysis between 2002/2003 and 2014/2015 (November to March), we used a total of 143,000 MODIS swaths for the complete Arctic domain, averaging at 73 scenes per day. The average amount of MODIS scenes per day and polynya region is additionally listed in Tab. 1.

2.2 ERA-Interim atmospheric reanalysis data

In order to provide the necessary atmospheric input for the applied surface energy balance model, the following variables from the European Center for Medium-Range Weather Forecasts (ECMWF) ERA-Interim reanalysis product (Dee et al., 2011) are

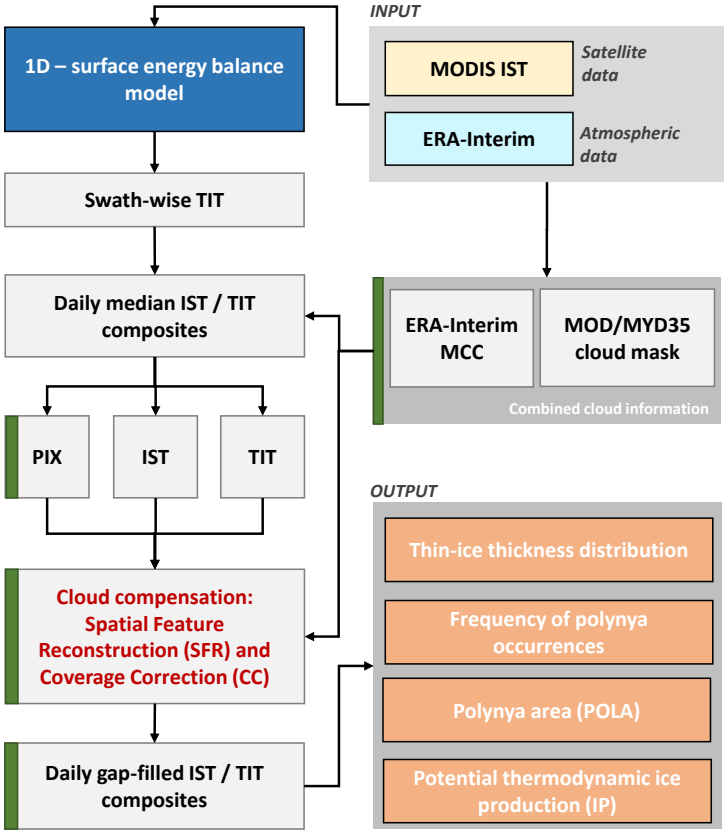

Figure 2. Schematic overview on the current version of the MODIS thin-ice thickness (TIT) retrieval scheme, based on Paul et al. (2015b) and Preußer et al. (2015a). The most recent updates are ~~highlighted~~ marked in ~~orange~~ green and are mainly aimed towards an additional cloud-cover treatment. Besides indicated abbreviations, 'IST' ~~denotes to~~, 'MCC' and 'PIX' denote the ice surface temperature, medium cloud cover and persistence index, respectively.

used: 2m-temperature, 2m-dew point temperature, 10m-wind speed and mean sea-level pressure. As the use of the ~~MOD35~~ MOD/MYD35 cloud mask during nighttime often ~~inhibits~~ contains misclassifications and ambiguities from undetected clouds and sea smoke, we additionally utilize ERA-Interim medium cloud cover (MCC) information. The study of Liu and Key (2014) demonstrated that the ERA-Interim MCC fields correspond closely to the MODIS derived cloud patterns throughout the seasons and can therefore be used as an additional quality control during the TIT retrieval. The temporal resolution of all variables is 6 h, so that each single MODIS swath can be linked to the closest time step of the atmospheric fields from ERA-Interim for the calculation of thin-ice thickness, with the overall average time difference being 90 ± 52 minutes (max. 180 minutes). The data set is provided by ECMWF at a spatial resolution of 0.75° (approx. 80 km). All ERA-Interim data fields are linearly interpolated and projected on the common reference grid in order to match the higher spatial resolution of MODIS data.

3 Methodology

3.1 MODIS thin-ice thickness retrieval using a surface energy balance model

We derive daily TIT distributions up to 50 cm by using an approach that follows the work of Yu and Rothrock (1996), Yu and Lindsay (2003) and Drucker et al. (2003). The core of this approach is an one-dimensional energy balance model, in which ice surface temperature (IST) and the thin-ice thickness are related to atmospheric radiation fluxes and turbulent heat fluxes. The original method of Yu and Rothrock (1996) was first improved and modified by Willmes et al. (2010) and Adams et al. (2013). More recently, the latest modifications of the algorithm are described in detail in Preußer et al. (2015b, a) and Paul et al. (2015b), together with comprehensive information on applied parametrization schemes that are used to calculate atmospheric radiation fluxes and turbulent heat fluxes. A complete overview on the currently used data-processing chain is given in Fig. 2.

There are certain limitations and simplifications attached to this procedure to derive TIT. First, it is only applicable to clear sky conditions, as clouds and sea smoke would strongly alter the recorded IST (Riggs et al., 2006). Second, we only use nighttime scenes to avoid potential ambiguities from incident short-wave radiation (Yu and Lindsay, 2003; Adams et al., 2013). Furthermore, newly formed ice is assumed to be free of snow and the temperature profile between the surface (IST) and the lower boundary of the ice (constant; freezing point of sea water) is linear. Consequently and following this assumption, the approach does not explicitly discriminate between different ice types within a polynya, as TIT are solely derived from calculating the heat conduction in/through ~~the~~ an assumed layer of ice (aside from subsequent gap-filling; see Sect. 3.2).

The study of Adams et al. (2013) presented a sensitivity analysis of the TIT retrieval, which revealed average uncertainties of $\pm$ 1.0 cm, $\pm$ 2.1 cm and $\pm$ 5.3 cm for TIT classes 0–5 cm, 5–10 cm and 10–20 cm, respectively. Between 20–50 cm, the uncertainty increases considerably. Therefore, we constrain our analysis accordingly as a thickness range of TIT $\leq$ 0.2 m is widely regarded as a threshold for polynya areas and for estimates of thermodynamic ice production in polynyas (Yu and Rothrock, 1996; Adams et al., 2013; Haid et al., 2015).

3.2 Calculation of daily TIT composites and correction of cloud- and data gaps

Because of the restriction to nighttime scenes, a less frequent MODIS coverage is present ~~in the beginning (November) and at the end (~~especially towards the end (February to March) of each winter-season. In order to increase the MODIS coverage for all considered areas (Fig. 1), we derive daily composites of IST and TIT from the total number of available MODIS swaths covering the Arctic domain on a given day (compare Sect. 2.1). Following the procedure described in Sect. 3.1, the TIT is first calculated from each single swath on its own. Subsequently, the daily median TIT per pixel is calculated and stored alongside its corresponding IST value and daily ~~averaged~~ median energy-balance components. The median is preferred over a simple average in order to reduce the potential risk of erroneously high or low values in single swaths, originating e.g. from unidentified clouds.

As described in Sect. 2.2, we additionally make use of ERA-Interim MCC fields as an indicator for potential cloud-coverage during the generation of daily TIT composites. Previous studies showed that a threshold of 75 % cloud-cover in the MCC-fields is quite effective in identifying and filtering/removing potentially cloud-affected areas (Paul et al., 2015b; Preußer et al., 2015a).

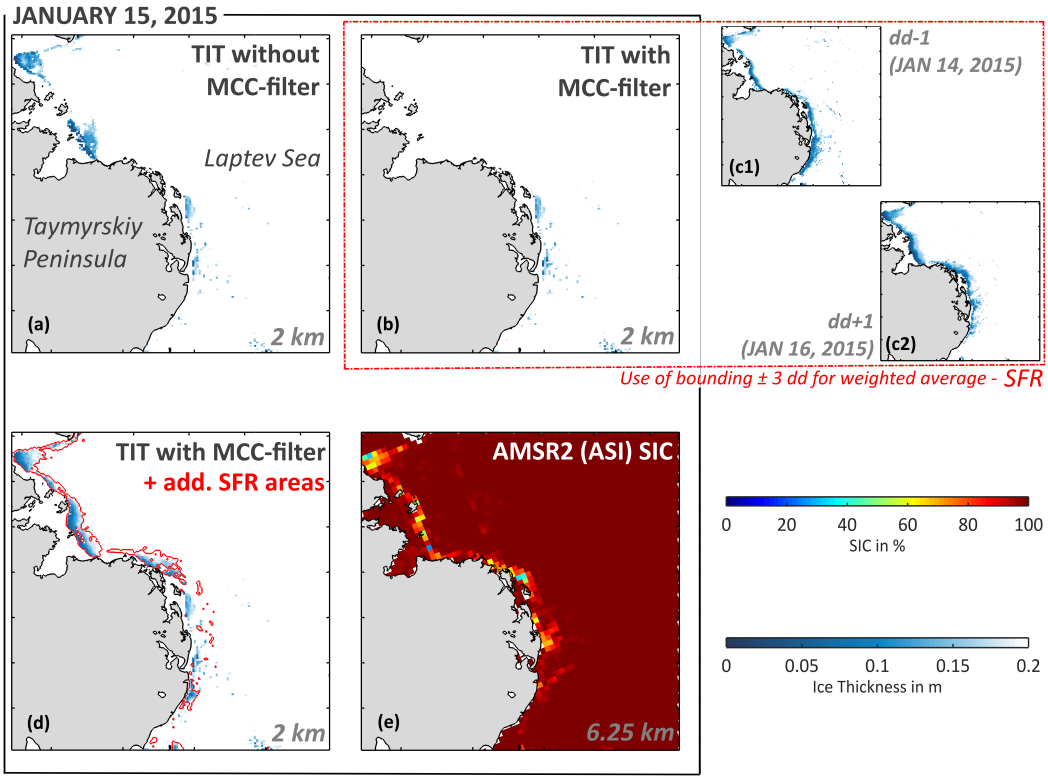

Figure 3. Different stages in the MODIS thin-ice thickness (TIT up to 0.2 m) processing chain for a single exemplary day (January 15, 2015). Sub-panels (a), (b), (c1/c2) and (d) all feature a subset (north-western Laptev Sea) from daily pan-Arctic TIT composites, with (a) showing the daily TIT without any cloud-treatment besides the MOD35 cloud mask and (b) the resulting TIT distribution after applying the ERA-Interim medium cloud cover (MCC) filter. Two bounding days with a better coverage of TIT are featured in panels (c1) and (c2) as a reference for the highest relative contribution in the spatial feature reconstruction (SFR) algorithm. The resulting spatial distribution of TIT after application of SFR is shown in panel (d), with new additional / reconstructed areas (up to 20 cm) marked in red. A comparison with Advanced Microwave Scanning Radiometer-2 (AMSR2) ASI sea-ice concentrations (Spreen et al. (2008); Beitsch et al. (2014); University of Bremen) from the same date is given in (e). The respective grid-resolution is given in the lower right corner of each sub-panel.

The combined MODIS and ERA-Interim cloud information allows for the assignment of four different quality-classes for each pixel in the daily composites: (1) confident clear-sky pixels ('ccs'; clear-sky MODIS and ERA-Interim), (2) mixed-covered pixels ('mcp'; ratio between clear-sky input swaths and the total number of input swaths per pixel), (3) definitive cloud-covered pixels ('dcc'; both in MODIS and ERA-Interim) and (4) completely uncovered pixels ('ucp').

Paul et al. (2015b) introduced an additional cloud-cover check based on the daily persistence of each pixel that is classified as thin ice (TIT ≤ 0.2 m). Misclassified thin-ice detections (i.e. clouds) are generally associated with low persistence-values due to their more mobile nature and displacements on sub-daily time scales. In contrast, polynyas show a higher spatial and temporal persistence due to their distinct formation mechanisms (Sect. 1). Leads, however, may be discarded by this criteria, since they generally have a low persistence due to their short lifetime and sea-ice drift caused by wind, ocean currents and tides. Based on these simple but distinct relations, we use a pixel-wise persistence index (PIX), defined as the ratio between the total number of MODIS swaths that feature thin-ice at a given pixel-location and the total number of swaths that feature clear-sky conditions at the same pixel-position.

All derived quality attributes (MCC-filter, cloud-cover information, PIX) are utilized in the Spatial Feature Reconstruction (SFR) algorithm (Paul et al., 2015a), which was recently successfully applied on a regional scale in both the Antarctic and Arctic to increase the information about otherwise cloud-covered areas (Paul et al., 2015b; Preußer et al., 2015a). The basic principle is that cloud-induced gaps in the daily TIT composites are compared with the TIT of the surrounding six days. In doing so, a probability of thin-ice occurrence is derived using a weighted composite of the days surrounding an initial day of interest (DOI). As in previous studies, we applied the following set of weights: w_3 = 0.02 (DOI $\pm$ 3), w_2 = 0.16 (DOI $\pm$ 2) and w_1 = 0.32 (DOI $\pm$ 1). The probability threshold remains fixed at th = 0.34 and needs to be surpassed in order to assign 'new' probable polynya pixels. Paul et al. (2015a) showed that this combination is less restrictive in terms of missing MODIS coverage in close proximity of the initial DOI. The procedure is applied on all areas with identified low-quality data (low persistence, cloud-covered), so that indicated gaps can be filled with new information on potential thin-ice occurrences. For these areas, new TIT and IST values are pixel-wise allocated using a weighted average ~~of~~ (same set of weights w_1 to w_3 applied) of the surrounding six days (Paul et al., 2015b; Preußer et al., 2015a). Table 1 gives an overview on the achieved MODIS coverage before and after application of the SFR algorithm. On a pan-Arctic level, the average (2002/2003 to 2014/2015) MODIS coverage is increased from around 0.75 (confident clear-sky and high-quality mixed-cover pixels featuring clear-sky conditions in more than 50% of all daily input swaths) to 0.93 (including SFR areas), with certain regions performing better (e.g. CBP, LAP, NEW, SZN) and some other regions noticeably worse (CHU, GLN, WNZ).

A total of 66 case studies in the Brunt Ice Shelf region of Antarctica demonstrated the generally good performance of the algorithm in comparison to more intelligible approaches by realistically reproducing artificially cloud covered thin-ice areas with an average spatial correlation of 0.83 and a RMSE of 1904 km^2 (Paul et al., 2015a). When compared to reference runs based on equally-weighted and in some cases shorter time intervals, the SFR procedure featuring above listed weights ~~w_3 to~~ w_1 to w_3 (DOI $\pm$ 3 days) yielded superior results both in spatial correlation and reconstructed ~~POLA-values~~polynya extent, regardless of the temporal polynya evolution (e.g. opening/closing events). As an additional example from the Arctic (north-western Laptev Sea), Fig. 3 visualizes the basic principle of the SFR algorithm, together with a qualitative comparison of Advanced Microwave

Table 1. Areal extents (i.e. total ocean area) of all applied polynya masks in km^2. Further, the interannual average amount of MODIS swaths that could be used for calculating daily composites in a given region is indicated, together with the interannual average daily MODIS coverage (decimal cover fraction ranging from 0 to 1 with their respective standard deviations) before (COV2) and after (COV4) application of the Spatial Feature Reconstruction (SFR) for each polynya region from 2002/2003 to 2014/2015 (November to March). The abbreviation 'ccs' denotes to confident clear-sky coverage, while 'HQ mcp' are high-quality mixed-cover pixels where either MODIS or ERA-Interim medium cloud cover feature cloud signals in the daily composites. In addition, the average thin-ice thickness (TIT, in cm) inside each polynya region (for all TIT ≤ 0.2 m) is given together with its standard deviation. An overview on all applied predefined polynya masks is given in Fig. 1.

Region	*Total ocean area*	*Avg. number of MODIS swaths*	*COV2*	*COV4*	*Avg. TIT*
	($10^3\mathrm{km}^2$)	(d^{-1})	(ccs, HQ mcp)	(ccs, HQ mcp, SFR)	(cm)
Beaufort Shelf (BSH)	91.6	6	0.76 ± 0.03	0.97 ± 0.02	14.0 ± 0.5
Canadian Arctic Archipelago (CAA)	719.6	14	0.82 ± 0.03	0.96 ± 0.01	13.7 ± 0.2
Cape Bathurst (CBP)	311.6	10	0.81 ± 0.03	0.98 ± 0.01	14.1 ± 0.4
Chukchi Sea (CHU)	286.0	5	0.55 ± 0.04	0.79 ± 0.03	12.8 ± 0.4
East Siberian Fast-Ice (ESF)	110.1	8	0.77 ± 0.04	0.96 ± 0.01	14.3 ± 0.3
East Siberian Sea (ESS)	904.1	9	0.70 ± 0.03	0.92 ± 0.01	14.0 ± 0.3
Franz-Josef-Land (FJL)	140.1	13	0.79 ± 0.04	0.97 ± 0.02	11.7 ± 0.8
Greenland North (GLN)	33.8	13	0.67 ± 0.04	0.81 ± 0.04	16.3 ± 0.4
Kara Sea (KAR)	725.5	14	0.75 ± 0.04	0.95 ± 0.02	11.7 ± 1.1
Laptev Sea (LAP)	281.1	12	0.80 ± 0.03	0.98 ± 0.01	13.5 ± 0.5
North East Water (NEW)	112.0	13	0.81 ± 0.03	0.98 ± 0.01	13.7 ± 0.5
North Water (NOW)	110.1	13	0.85 ± 0.04	0.97 ± 0.01	11.5 ± 0.5
Nares Strait / Lincoln Sea (NSL)	55.5	14	0.83 ± 0.03	0.96 ± 0.01	13.6 ± 1.0
Storfjorden (STO)	11.7	9	0.75 ± 0.04	0.95 ± 0.03	9.2 ± 1.7
Svalbard Archipelago (SVA+STO)	204.3	13	0.68 ± 0.06	0.90 ± 0.04	7.2 ± 1.0
Severnaya Zemlya North (SZN)	65.3	12	0.80 ± 0.04	0.98 ± 0.01	13.5 ± 0.6
Western Novaya Zemlya (WNZ)	211.6	12	0.60 ± 0.07	0.83 ± 0.04	6.8 ± 1.6
Total	436.2	73[a]	0.75 ± 0.04	0.93 ± 0.02	12.7 ± 0.6

a Not the sum of all regions, as single MODIS swaths may cover multiple regions at the same time.

Scanning Radiometer 2 (AMSR2) sea-ice concentration (SIC) data (Spreen et al., 2008; Beitsch et al., 2014). As a first step, the MCC-filter eliminates potentially cloud-influenced areas which are in this case located north of the Taymyr Peninsula (Laptev Sea, Russia). One could argue that this filtering is a bit harsh, but we choose a more conservative threshold to minimize the risk of 'false' thin-ice pixels. Afterwards, the SFR algorithm is applied and a new gap-filled TIT composite (Fig. 3 (d)) is produced. In this particular example from January 15, 2015, the reconstructed TIT distribution compares well with locations of lower SIC from AMSR2 (Fig. 3 (e)) while maintaining the increased spatial detail at the same time. Based on this example and successful applications in previous works by the authors (Paul et al., 2015a, b; Preußer et al., 2015a), we conclude that the applied schemes to compensate and correct cloud-effects work reasonably well on a pan-Arctic scale and allow for a fair comparison to other commonly used remote sensing approaches to infer polynya characteristics, with limitations regarding the reconstruction of leads.

3.3 Derivation of ice production and polynya area

Ice production rates are derived by assuming that the entire heat loss at the ice surface to the overlying atmosphere contributes to new ice formation (Tamura et al., 2007, 2008; Willmes et al., 2011). Components for the following equation (Eq. 1) can be taken from calculated and gap-filled daily MODIS composites.

$$\frac{\partial h}{\partial t} = \frac{-\bar{Q}_{ice}}{\rho_{ice} * L_f} \tag{1}$$

Therein, $\frac{\partial h}{\partial t}$ denotes to the ice production rate, $\bar{Q}_{ice}$ is the daily mean conductive heat flux through the ice, ρ_{ice} is the density of the ice (ρ_{ice} = 910 $\mathrm{kg/m^3}$; Timco and Frederking (1996)) and L_f is the latent heat of fusion of sea ice (L_f = 0.334 $\mathrm{MJ/kg}$; Tamura and Ohshima (2011)). Concerning L_f, Tamura and Ohshima (2011) noted that an accurate value for areas of high ice production is not known so far. Following the work of Martin (1981), Tamura and Ohshima (2011) argued that frazil ice consists of freshwater ice crystals enclosed with a thin saline layer and that frazil ice production rates are of similar magnitudes as freshwater ice production rates. Consequently, we also use fixed values for ρ_{ice} and L_f in order to ensure comparability with earlier studies focusing on sea-ice production in (Arctic) polynyas (e.g. Willmes et al., 2011; Tamura and Ohshima, 2011; Iwamoto et al., 2014). However, this simplification may introduce an additional error source in our estimates due to spatially and temporally varying conditions for ice formation. Note that the negative sign in Eq. 1 implies that the atmospheric heat flux is positive when the surface gains energy, and at the same time it assures that ice production only takes place when there is a net energy loss from the surface. According to the surface energy balance, the heat flux $\bar{Q}_{ice}$ is equal to the total atmospheric heat loss (sum of net radiation, turbulent latent and sensible heat flux). We do not consider an ocean heat flux, although it might potentially reduce thermodynamic ice growth in certain areas of the Chukchi Sea (Hirano et al., 2016), the Canadian Arctic Archipelago (Hannah et al., 2009; Melling et al., 2015) and northern Baffin Bay (e.g. Steffen, 1985; Yao and Tang, 2003) by as much as 23-27% in case of the NOW polynya (Tamura and Ohshima, 2011; Iwamoto et al., 2014). The volume ice production rate $\frac{\partial V}{\partial t}$ (*IP*) is calculated by multiplying $\frac{\partial h}{\partial t}$ with the areal extent of each pixel in the regarded region. Ice production rates are calculated for each pixel with a TIT $\leq$ 0.2 m and afterwards extrapolated to daily rates. However, it has to be noted that daily

IP rates inhibit a positive bias due to the exclusive use of both nighttime and clear-sky MODIS scenes. The former is mainly of concern during the late autumn / early spring period when polar night conditions are absent, while the latter circumstance is unavoidable throughout each winter when relying on optical and infrared remote sensing data. Since low-level clouds reduce the net radiative loss by about 50 $\mathrm{W/m^2}$ in polar regions (Heinemann and Rose, 1990; König-Langlo and Augstein, 1994), the restriction to cloud-free conditions in the daily composites results in a positive bias in IP. ~~Considering the fraction of average MODIS coverage of 75% (COV2; Tab. 1)~~ Considering an average clear-sky fraction of 73 $\pm$ 8 % per pixel from all input swaths in a given daily composite and assuming that not all clouds are low-level, the overestimation of net energy loss by our method can be estimated to be less than 10 $\mathrm{W/m^2}$, which corresponds to less than 0.4 m IP per winter.

The daily polynya area (POLA, in $\mathrm{km^2}$) in each polynya mask (Fig. 1) is defined as the accumulated total area of all thin-ice pixels with a TIT $\leq$ 0.2 m. Remaining MODIS coverage gaps after the application of the SFR approach (e.g. prolonged periods of ~~stable~~ persistent cloud cover, i.e. no coverage on more than 3 consecutive days) are handled by additionally applying an extrapolation approach (coverage-correction; CC) on calculated POLA and IP estimates, which yields daily values with an error-margin of 5 to 6% (Preußer et al., 2015b). In case of very persistent cloud cover inside the respective reference areas and a resulting daily MODIS coverage below 50% (i.e. COV4 < 0.5), both daily POLA and IP are linearly interpolated from bounding days.

The complete period from November to March each winter is considered for the calculation of POLA / IP, which implies that the here derived values are potentially influenced by shifts in the timing of freeze onset during the early freezing season (November / December). For potentially MIZ-influenced regions (CHU, SVA, NOW, WNZ, KAR), this has to be considered when comparing metrics derived for the full winter period (November to March).

For topographically complex regions like Greenland and Arctic fjords, recent studies revealed shortcomings of the coarse-resolution ERA-Interim data regarding the representation of mesoscale spatial features in the wind field, such as tip-jets, channeling effects or other topography-induced phenomena related to locally increased wind speeds (e.g. Moore et al., 2016). Thus, ERA-Interim shows a tendency to underestimate peak wind speeds (Moore et al., 2016) which might in some cases induce a negative bias (lower heat fluxes/ smaller POLA / less IP) in regions where polynya formation is strongly influenced by the local topography (e.g. CAA, NOW, NEW, SZN). In our study, the usage of ERA-Interim is motivated by ensuring comparability to similar studies (e.g. Iwamoto et al., 2014) as well as the constraint that higher-resolution atmospheric data sets such as the Arctic System Reanalysis (ASRv1 – 30km; Bromwich et al., 2015) are currently not available for the complete time period from 2002 to 2015.

4 Results and Discussion

4.1 Thin-ice dynamics, polynya area and thermodynamic ice production in the Arctic for 2002/2003–2014/2015

Interannual average values for TIT $\leq$ 0.2 m are listed in Tab. 1 for each polynya region. They range between 6.8 cm (WNZ) and 16.3 cm (GLN), with an overall average of about 12.7 $\pm$ 0.6 cm. The underlying long-term time series of average wintertime

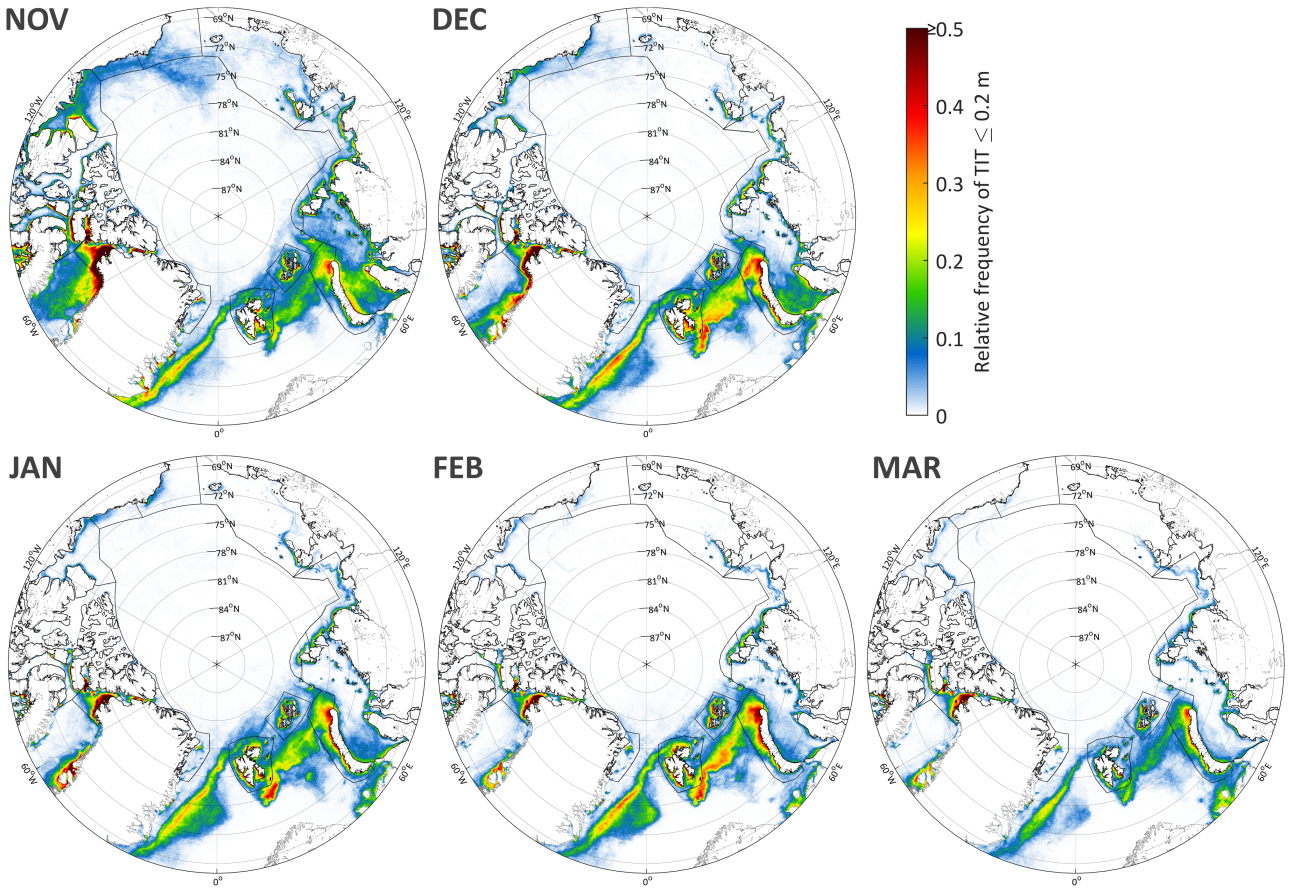

Figure 4. Average wintertime (November to March) frequencies of TIT $\leq$ 0.2 m in the Arctic between winters 2002/2003 and 2014/2015. For each month, frequencies are calculated per pixel as the fraction of days with a TIT $\leq$ 0.2 m relative to the 13-yr investigation period. Note that only thin-ice areas within the margins of a given polynya mask (dashed black lines; compare Fig. 1) are used for further analysis, while all other areas are discarded. Hence, areas with high TIT frequencies in the marginal ice zone (MIZ) around Fram Strait and northern Barents Sea are excluded from further analysis due to potential ambiguities originating from ocean heat fluxes and a high interannual variability of the MIZ in terms of location and extent.

TIT within each polynya (not shown) reveal a tendency towards decreasing thin-ice thicknesses in almost every region (e.g. up to 2.5 cm per decade in the Storfjorden polynya), with the only exceptions being the CAA, GLN and NEW.

~~Thin-ice frequencies of~~ Monthly thin-ice frequencies, calculated per pixel as the fraction of days with a TIT $\leq$ 0.2 m relative to the 13-yr investigation period, are presented in Fig. 4. Frequencies of larger than 0.5 are primarily found around the Canadian Arctic, first and foremost in the North Water (NOW) polynya and the eastern CAA ~~(Fig. 4).~~ . More specifically, coastal areas around Devon Island and south-eastern Ellesmere Island (Hells Gate / Cardigan Strait) and larger areas at the eastern exits of Lancaster Sound and Jones Sound are well visible and have previously been related to tidal currents and slightly increased

ocean heat fluxes (Hannah et al., 2009; Melling et al., 2015). Other areas with similar magnitudes include the Storfjorden polynya and coastal areas (north-)west of Novaya Zemlya. Besides, elongated thin-ice areas along the Siberian shelf (Laptev and Kara Sea; frequencies around 0.05 to 0.35 each month) are well delineated. Locations of frequent thin-ice occurrences in the Kara Sea are in accordance with results from the study of Kern (2008). The northern Barents Sea, Franz-Josef-Land and the Svalbard archipelago also feature quite high appearance rates of around 0.1 to 0.3. Contrary to earlier reports (Barber and Massom, 2007), the North-East Water (NEW) polynya in north-eastern Greenland (approx. 81° N, 13° W) neither shows any sign of disappearance, nor is it limited to the spring to late autumn period. With average frequencies of around 0.1 to 0.25 each month in winter, it has more likely to be categorized as a regularly forming polynya. Comparatively low frequencies below 0.15 (especially from January to March) are primarily found in the Beaufort and Chukchi Sea as well as in the East Siberian Sea. Vast fast-ice areas, e.g. along the Siberian coast, can be detected from monthly TIT frequencies, as these areas usually appear at fixed locations attached to the shore and TIT frequencies tend towards zero as the ice quickly thickens by congelation ice growth. Hence, our 13-year record of monthly TIT-occurrence rates offers the potential to further develop optimized automatic methods for a regular Arctic-wide mapping of monthly fast-ice extents and could thereby ~~compliment~~ complement currently existing approaches from earlier studies (e.g. Yu et al., 2014; Mahoney et al., 2014; Selyuzhenok et al., 2015).

Compared to the study of Willmes and Heinemann (2016), leads are only weakly visible in ~~this~~ these long-term averages (frequencies below 0.05–0.1). In Fig. 4, leads are mainly located in the area of the Beaufort Sea and north of Greenland (shear zones) which can be mainly attributed to their relatively high spatial and temporal persistence. Frequent lead occurrences in e.g. the East-Siberian Sea found by Willmes and Heinemann (2016) are not reflected in our study. In some regions, however, the influence of (shelf-) bathymetry and associated ocean currents on the spatial distribution of polynya and lead occurrences is also visible in our here derived TIT frequencies (e.g. eastern exit Vilkitsky Strait, Hanna Shoal / northern Chukchi Shelf, northern ESS).

In Fig. 5 and Fig. 6, the interannual variability of the average POLA (in km^2) and accumulated IP (in km^3) are presented for all examined polynya regions, respectively. In both figures, the difference between the beginning (November to December) and end (January to March) of the freezing (winter) period is additionally highlighted. Concerning POLA, it shows that the largest average wintertime extents are found in the NOW, WNZ and KAR areas. The study of Preußer et al. (2015a) demonstrated that the large POLA values in the NOW-region are part of a (non-significant) long-term increase of average polynya extents between 1978 and 2015. In case of polynyas in proximity of Novaya Zemlya, the here derived average wintertime value for POLA of around 42 x 10^3 km^2 is fairly close to the respective value by Iwamoto et al. (2014) (49 x 10^3 km^2), despite the circumstances that their study covers an extended winter period from September to May and features a different mask area, which stretches over some part of the western Kara Sea. As mentioned earlier, Kern (2008) presented POLA values for the Kara Sea. His retrievals are based on approximately the same reference area (Fig. 1), which in this case allows for a fair comparison to the here presented numbers. It shows that the average POLA in the late freezing season reveals similar magnitudes in recent years. During the period from 1979 and 2004, the average POLA (in Kern (2008): January to April) ranged between 1 to 5 x 10^4 km^2 (except for 1995: around 6 x 10^4 km^2), which is close to the range of our here presented results for January to March (Fig.5; Tab. 2). Although the estimated positive trend in POLA remains non-significant for the Kara Sea as in Kern (2008), the

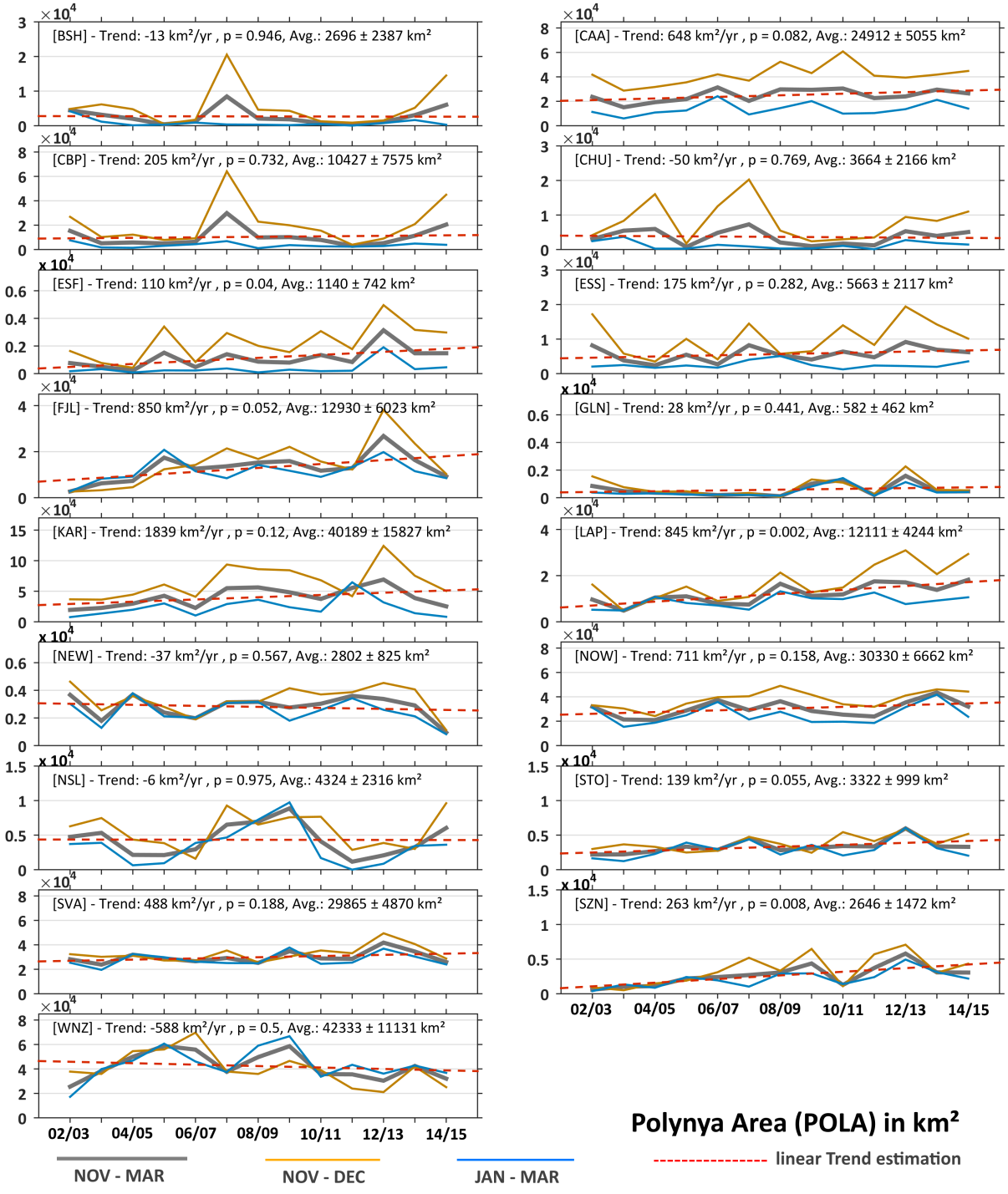

Figure 5. Regional time series of the annual average polynya area (POLA; TIT ≤ 0.2 m) in km^2 for 2002/2003 to 2014/2015, together with a seasonal comparison (November to December vs. January to March) and a linear trend estimation. The estimated linear trend (in km^2/yr), its p-value and the interannual average POLA (in km^2) are additionally listed in each sub-panel. Please note the varying scale on each y-axis.

Figure 6. Regional time series of the annually accumulated ice production (IP) in km^3 for 2002/2003 to 2014/2015, together with a seasonal comparison (November to December vs. January to March) and a linear trend estimation. The estimated linear trend (in km^3/yr), its p-value and the interannual average IP (in km^3) are additionally listed in each sub-panel. Please note the varying scale on each y-axis.

Table 2. Average polynya area (POLA) in km^2 in each polynya region between 2002/2003 and 2014/2015 (SFR cloud-cover correction applied). Besides being based on the available winter period from November to March, it is further separated between the early freezing season (November to December) and the late freezing season (January to March). All values are derived from daily MODIS TIT composites after application of the predefined polynya masks (Fig. 1). Trends are additionally given, where underlined, bold and bold italic numbers denote statistical significance (two-sided t-test) at the 90, 95 and 99 % level, respectively.

	November to March		November to December		January to March	
Region	*Avg. POLA* ($10^3\mathrm{km}^2$)	*Trend POLA* ($\mathrm{km}^2/\mathrm{yr}$)	*Avg. POLA* ($10^3\mathrm{km}^2$)	*Trend POLA* ($\mathrm{km}^2/\mathrm{yr}$)	*Avg. POLA* ($10^3\mathrm{km}^2$)	*Trend POLA* ($\mathrm{km}^2/\mathrm{yr}$)
Beaufort Shelf (BSH)	2.7 ± 2.4	-13	5.5 ± 5.8	132	0.8 ± 1.1	-111
Canadian Arctic Archipelago (CAA)	24.9 ± 5.1	648	41.5 ± 8.3	958	13.7 ± 5.2	438
Cape Bathurst (CBP)	10.4 ± 7.6	205	20.6 ± 16.9	581	3.6 ± 2.0	-49
Chukchi Sea (CHU)	3.7 ± 2.2	-50	8.2 ± 5.7	-95	1.3 ± 1.1	-37
East Siberian Fast-Ice (ESF)	1.1 ± 0.7	**110**	2.3 ± 1.3	**200**	0.4 ± 0.5	48
East Siberian Sea (ESS)	5.7 ± 2.1	175	10.3 ± 5.2	385	2.5 ± 1.1	33
Franz-Josef-Land (FJL)	12.9 ± 6.0	850	15.2 ± 9.7	**1565**	11.5 ± 4.9	380
Greenland North (GLN)	0.6 ± 0.5	28	0.8 ± 0.6	14	0.5 ± 0.4	37
Kara Sea (KAR)	40.2 ± 15.8	1839	64.9 ± 26.8	3209	23.5 ±15.5	904
Laptev Sea (LAP)	12.1 ± 4.2	***845***	17.0 ± 8.0	***1559***	8.8 ± 2.7	362
North East Water (NEW)	2.8 ± 0.8	-37	3.3 ± 1.0	-10	2.4 ± 0.9	-55
North Water (NOW)	30.3 ± 6.7	711	37.7 ± 7.1	**1072**	25.4 ± 7.8	464
Nares Strait / Lincoln Sea (NSL)	4.3 ± 2.3	-6	5.7 ± 2.6	18	3.4 ± 2.8	-22
Storfjorden (STO)	3.3 ± 1.0	139	3.9 ± 1.1	**175**	2.9 ± 1.3	115
Svalbard Archipelago (SVA+STO)	29.9 ± 4.9	488	32.8 ± 6.5	732	27.9 ± 5.3	327
Severnaya Zemlya North (SZN)	2.6 ± 1.5	***263***	3.4 ± 2.2	**353**	2.1 ± 1.2	**203**
Western Novaya Zemlya (WNZ)	42.3 ± 11.1	-588	40.4 ± 13.8	-1806	43.6 ± 13.0	230
Total	226.6 ± 36.1	**5468**	309.4 ± 62.6	8864	171.3 ± 32.6	3151

magnitude of the trend in the late freezing period (January to March; around 9000 km^2/decade) seems to have increased from 2400 km^2/decade (Kern, 2008) to around 9000 km^2/decade over the last 13 years. The interannual POLA variability in all regions is generally pronounced, but is especially large for smaller polynyas / thin-ice regions such as the NSL, NEW and ESS. Concerning seasonal differences, it appears that some regions (e.g. NEW, GLN, LAP, SZN) have the tendency towards larger thin-ice areas during the freeze-up period since approximately 2006/2007 to 2007/2008. About 8 to 10 polynya regions show distinct positive trends of up to 18,390 km^2 per decade (KAR), with only the LAP, ESF and SZN regions being significant (two-sided t-test) with $p \leq 0.05$. Interestingly, sub-regions located in proximity of the Beaufort Gyre (BSH and CBP) indicate very large thin-ice areas between November and December 2007, shortly after the 2nd lowest September sea-ice extent since 1979 (approx. 4.7 million km^2; Parkinson and Comiso (2013)). This did not appear in a similar way in 2012 (record low of approx. 3.4 million km^2). A detailed investigation shows that the freeze-up in the Beaufort Sea area was much slower in 2007 and extended until mid-December, while in 2012 the same area was ice-covered by November 10. The study of Timmermans (2015) linked this significant delay in ice growth to upward mixing processes of ocean heat in the Canada Basin, originating from the release of stored solar heat input following summer 2007. This resulted in large areas with very thin ice (around

Table 3. Average accumulated ice production (IP) in km^3 in each polynya region between 2002/2003 and 2014/2015 (SFR cloud-cover correction applied). Besides being based on the available winter period from November to March, it is further separated between the early freezing season (November to December) and the late freezing season (January to March). All values are derived from daily MODIS TIT composites after application of the predefined polynya masks (Fig. 1). Trends are additionally given, where underlined, bold and bold italic numbers denote statistical significance (two-sided t-test) at the 90, 95 and 99 % level, respectively.

	November to March		November to December		January to March	
Region	*Acc. IP* (km^3)	*Trend IP* (km^3/yr)	*Acc. IP* (km^3)	*Trend IP* (km^3/yr)	*Acc. IP* (km^3)	*Trend IP* (km^3/yr)
Beaufort Shelf (BSH)	23 ± 23	-0.5	19 ± 23	0.0	5 ± 5	-0.4
Canadian Arctic Archipelago (CAA)	215 ± 43	5.4	136 ± 23	2.5	79 ± 31	2.9
Cape Bathurst (CBP)	78 ± 54	1.0	60 ± 48	1.1	18 ± 10	-0.1
Chukchi Sea (CHU)	27 ± 16	-0.5	20 ± 14	-0.3	7 ± 6	-0.2
East Siberian Fast-Ice (ESF)	9 ± 5	**0.8**	7 ± 3	**0.6**	2 ± 2	0.3
East Siberian Sea (ESS)	41 ± 13	1.5	28 ± 13	1.3	13 ± 5	0.2
Franz-Josef-Land (FJL)	99 ± 41	5.6	42 ± 24	**4.1**	57 ± 22	1.5
Greenland North (GLN)	5 ± 4	0.2	3 ± 2	0.0	3 ± 2	0.2
Kara Sea (KAR)	277 ± 111	12.6	174 ± 76	9.0	104 ± 56	3.6
Laptev Sea (LAP)	96 ± 33	***6.8***	51 ± 24	***4.8***	45 ± 14	**2.0**
North East Water (NEW)	22 ± 7	-0.4	10 ± 3	0.0	12 ± 4	-0.4
North Water (NOW)	277 ± 67	6.0	135 ± 27	3.4	145 ± 45	2.6
Nares Strait / Lincoln Sea (NSL)	39 ± 22	0.1	20 ± 10	0.2	20 ± 16	-0.1
Storfjorden (STO)	21 ± 6	**0.9**	10 ± 4	**0.5**	11 ± 4	0.4
Svalbard Archipelago (SVA+STO)	214 ± 33	0.8	91 ± 24	1.6	123 ± 24	-0.8
Severnaya Zemlya North (SZN)	22 ± 11	***2.0***	10 ± 6	**0.9**	12 ± 6	**1.1**
Western Novaya Zemlya (WNZ)	367 ± 124	-7.0	136 ± 56	-6.8	231 ± 88	-0.2
Total	1811 ± 293	34.5	940 ± 178	22.4	871 ± 175	12.1

170,000 km^2) in November to December and consequently allowed for huge amounts of latent and sensible heat to be released from the ocean, leading to extraordinary high IP values in these areas (Fig. 6).

Regarding IP, many of the above described features are also visible in the regional time series of Fig. 6. Contrary to Tamura and Ohshima (2011), the majority of polynya regions shows overall positive (up to 126 km^3 per decade (KAR)) or no trends in wintertime ice production, and only four regions indicate a slight, yet insignificant decrease over the last 13 years (BSH, CHU, NEW, WNZ). Complete overviews on calculated average POLA and IP values per region, together with their respective trends, are given in Tab. 2 and Tab. 3, respectively. These overviews highlight that seasonal differences (November to December vs. January to March) have a huge effect on calculated average values and trends for the complete winter period from November to March. Consequently, the here discussed numbers should be regarded as winter integrals with potentially inherent effects originating from the timing of freeze-up onset. In case of e.g. the Kara Sea, Franz-Josef-Land, the Chukchi Sea ~~,~~ and the Canadian Arctic Archipelago~~and the Storfjorden polynya~~, large thin-ice and potential open-water areas during the early freezing period in November and December imprint on the total winter averages as well as derived trends of POLA and IP, especially

from 2007/2008 onwards. While the majority of polynyas also feature positive trends in the late freezing season from January to March, these trends are for the most part not significant.

The average total ice production in Arctic polynyas sums up to 1811 $\pm$ 293 km^3 per winter. Thus, it lies in between previously determined average values of 2940 $\pm$ 373 km^3 (Tamura and Ohshima, 2011; 1992/1993 - 2007/2008) and 1178 $\pm$ 65 km^3 (Iwamoto et al., 2014; 2002/2003 - 2010/2011) per winter. We expect that the MODIS-derived quantities offer a valuable increase in both spatial and quantitative accuracy due to the use of high-resolution and gap-filled daily fields of thin-ice thicknesses. A shortening of the averaging interval to the period 2002/2003 - 2010/2011 (as in Iwamoto et al. (2014), but not accounting for differences in covered winter period) reduces the here derived average total ice production marginally by about 1-2%. In order to assess apparent differences between our here derived data-set and the passive microwave data set by Iwamoto et al. (2014), a more direct comparison based on identical reference areas and the same winter period would be necessary.

A spatial overview of the average (2002/2003 to 2014/2015) accumulated ice production per winter (November to March) is presented in Fig. 7. Likewise to Fig. 4, the NOW polynya stands out at first glance due to its high average ice production of up to 14 m per winter. However, smaller polynyas in the Canadian Arctic (around Devon Island) feature comparatively high values for ice production. Most other areas in the Arctic produce on average between 1-3 m of ice per winter, with a few noticeable exceptions like Franz Josef Land (about 4-5 m per winter), the northern tip of Novaya Zemlya (5-7 m per winter) and some coastal areas in the Kara Sea (1-4 m per winter). While the core areas of high ice production show a high resemblance to Iwamoto et al. (2014) with marginal differences in absolute numbers, MODIS is capable to provide enhanced spatial detail. This is especially valuable concerning the narrow thin-ice areas along the coast and fast-ice edges in the eastern part of the Arctic (Kara Sea, Laptev Sea, East Siberian Sea), as these areas are not resolved by the coarse-resolution passive microwave data (6.25 km; Iwamoto et al., 2014). This striking advantage is also reflected in the comparatively narrow fjords and bays/sounds around Greenland and the Canadian Archipelago, where a high ice production of up to 3 meters per winter is found. While these observations, mostly related to differences in spatial resolution, could explain the above described discrepancy in average accumulated numbers to some extent (compare Preußer et al. (2015a)), the net effect of a lower grid size cannot be quantified here.

Spatial trends between the winter seasons 2002/2003 and 2014/2015 (November to March) can be calculated by applying a linear regression on the annual accumulated IP per pixel. The resulting map is shown in Fig. 8 (a). Besides many interesting small-scale patterns, two main conclusions can be drawn from this spatial overview: (1) While the trends identified in the western Arctic show no consistent pattern, large areas of the eastern Arctic are characterized by significant (two-sided t-test; significance levels indicated in Fig. 8 (b)) positive trends that can exceed 2 meters per decade and (2) ~~the spatial structure of~~ we observe opposing negative / positive IP-trends along the coasts of the Laptev ~~Sea and Kara Sea suggests a southward shift of the~~ and Kara Seas which could be due to changes in fast-ice ~~edge with potential implications for the fast-ice~~ extent over the ~~recent 13 years~~13-year period. Decreasing fast-ice extents and durations in the eastern Arctic between 1976 and 2007 were recently described by Yu et al. (2014). In addition, Selyuzhenok et al. (2015) analyzed the fast ice in the south-eastern Laptev Sea in more detail (1999 to 2013). While their study showed that the winter maximum fast-ice extent (March/April) as well

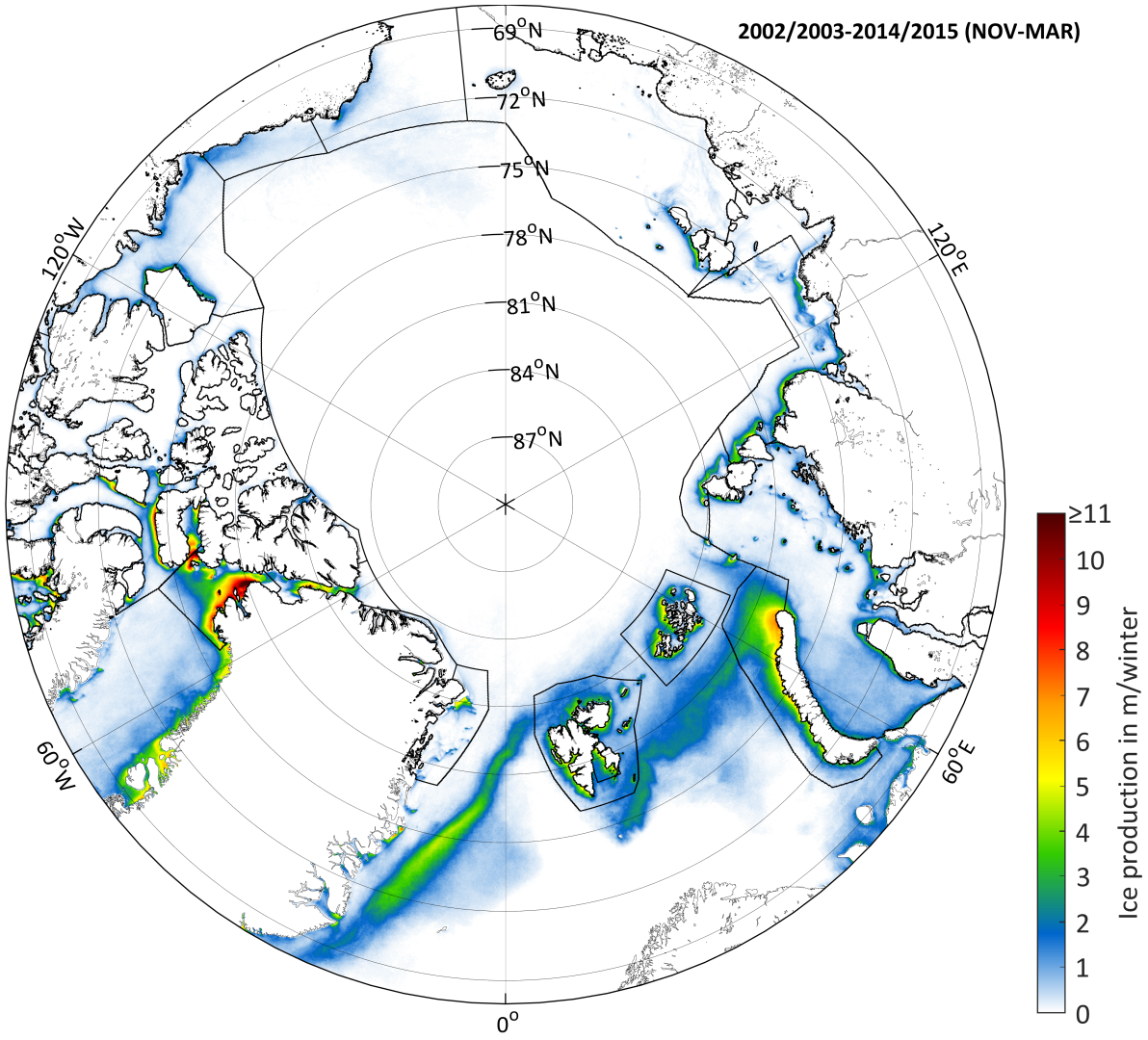

Figure 7. Average (2002/2003 to 2014/2015) accumulated ice production (m per winter) during winter (November to March) in the Arctic, north of 68° N. The margins of applied polynya masks (Fig. 1) are shown in black dashed lines.

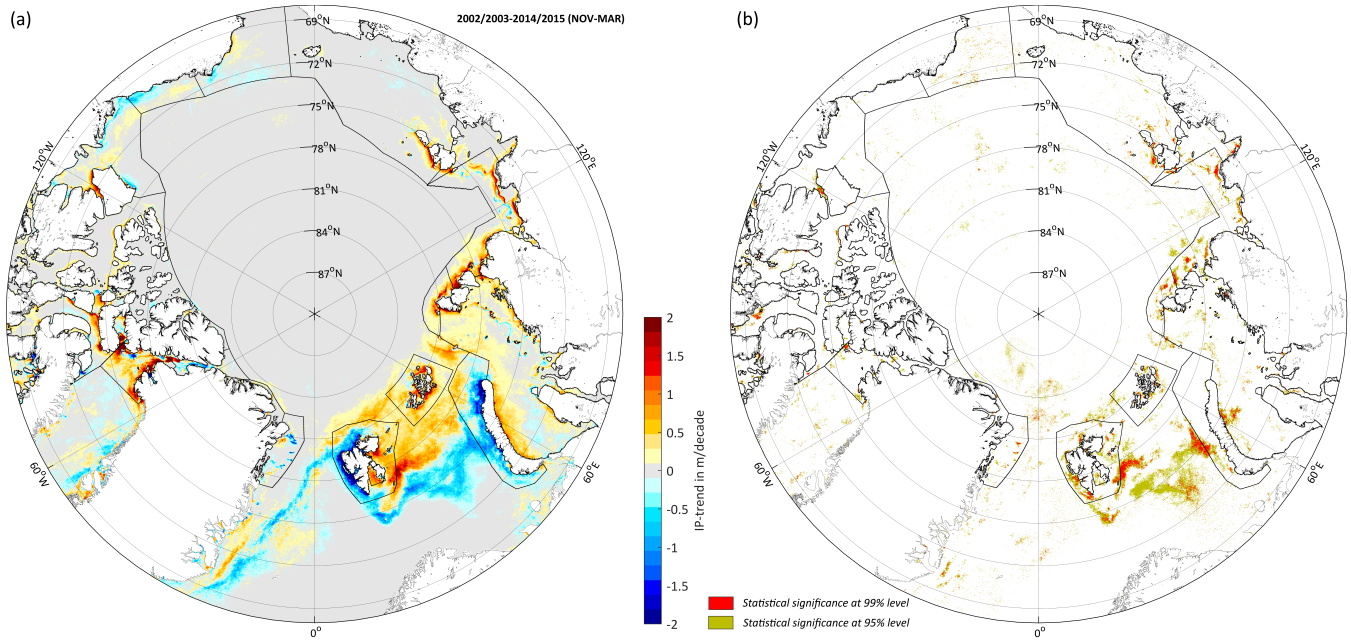

Figure 8. (a) Decadal trends (m per decade) of wintertime (November to March) ice production in the Arctic, north of 68° N. Trends are calculated by applying a linear regression on the annual accumulated IP per pixel for the period 2002/2003 to 2014/2015. Areas with statistical significance (based on a two-sided t-test) at the 95% and 99% level are depicted in (b). The margins of applied polynya masks (Fig. 1) are shown in black dashed lines.

as the shape and location of the fast-ice edge did not vary significantly over the regarded time period, they likewise presented an overall decrease in the fast-ice season (-2.8 $\mathrm{d/yr^{-1}}$) due to a later formation and earlier break-up. These described changes regarding the timing of fast-ice formation in early winter could explain the observed structures of positive / negative trends in proximity of fast-ice areas.

In order to put these observations into context, we suppose that this characteristic pattern of opposing trends in the western and eastern Arctic as well as the apparently fast-ice related structures in the Laptev Sea and Kara Sea could be connected to an overall later appearing fall freeze-up (Markus et al., 2009; Stroeve et al., 2014) in recent years, which itself is thought to result from a complex mixture/interplay of steadily and year-round increasing (2m-) air temperatures (e.g. Cohen et al., 2014), distinct large-scale atmospheric patterns (e.g. Rigor et al., 2002) and the overall downward trend of total sea-ice extent and volume in the Arctic (e.g. Schweiger et al., 2011; Laxon et al., 2013). The latter implies a tendency towards a more fragile, thus mobile, sea-ice cover in the Arctic, with a potentially increased sensitivity for external forcing mechanisms (i.e. strong winds and/or ocean currents) that are responsible for thin-ice formation in polynyas and leads. As being one of the main regions with highly pronounced and significant positive trends in both POLA and IP throughout the complete winter period, the following section will take a closer look on polynya dynamics in the Laptev Sea.

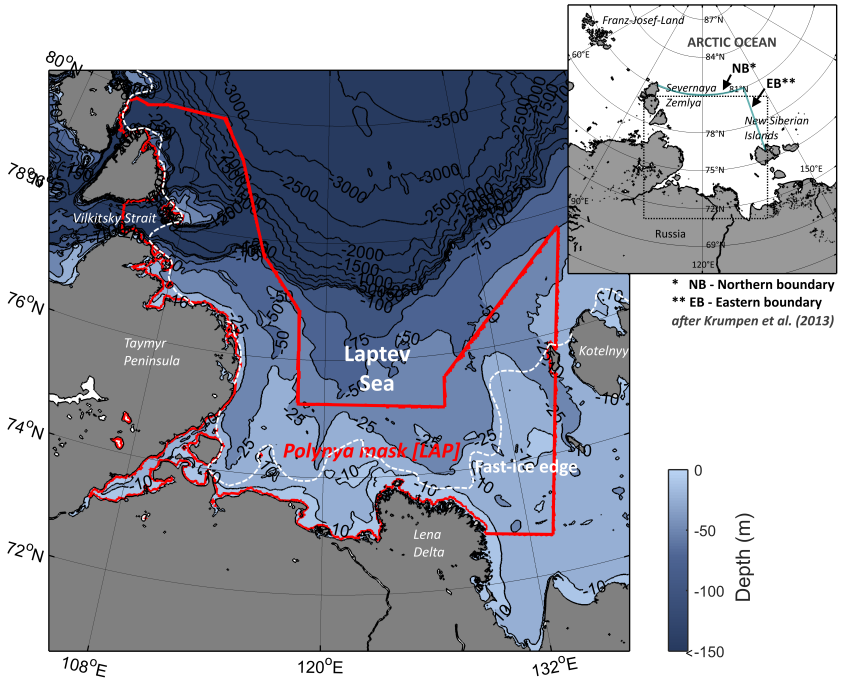

Figure 9. The geographical location of the Laptev Sea in the eastern Arctic. The applied polynya mask is marked in red, enclosing the locations of typical polynya formation along the coast and fast-ice edge (dashed white line; position derived from long-term thin-ice frequencies in March (Fig. 4)). Flux gates from the study by Krumpen et al. (2013) at the northern (NB) and eastern (EB) boundary of the Laptev Sea are shown in the inset map (cyan solid lines). Bathymetric data by Jakobsson et al. (2012) (IBCAO v3.0).

4.2 Regional focus - Laptev Sea

One main advantage of the high-resolution MODIS data is the ability to perform detailed investigations on a regional scale across the Arctic. The grid spacing of 2 km allows for the detection of relatively fine and delineated polynya structures and for more accurate statements about areas of high ice production, as it was previously possible.

The Laptev Sea was previously described as a key region to investigate climatic changes in the Arctic shelf seas (ACIA, 2005), as it is one of the major source area for sea ice export into the Transpolar Drift system (Dethleff et al., 1998). As can be seen in Fig. 9, the Laptev Sea is located between the Severnaya Zemlya at the western boundary, the Lena Delta at the southern edge and the New Siberian Islands, which serve as the boundary in the East (approximately 70-80°N, 100-140°E). The water-mass composition in the Laptev Sea is temporarily quite variable, as there is a huge freshwater inflow during the summer and autumn period (around 750 km^3 per year; Rigor and Colony (1997)) and strong ice-formation accompanied with brine rejection in polynyas during winter (Bauch et al., 2012). These processes significantly alter the stratification of the upper ocean layers as well as the salinity levels in the annual cycle. These and other recurring features of the sea ice and ocean environments have recently been illustrated and updated by Janout et al. (2016).

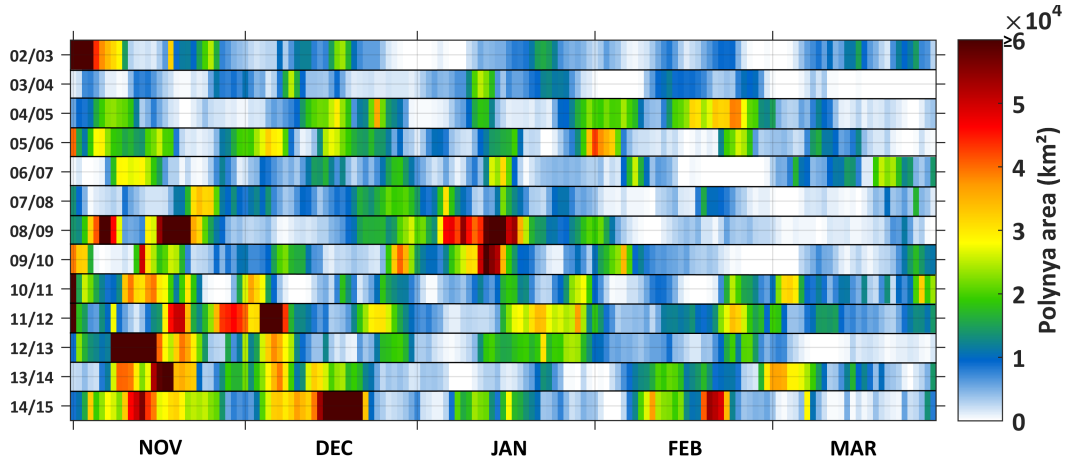

Figure 10. The daily polynya area (TIT $\leq$ 0.2 m) in the Laptev Sea region for the winter seasons 2002/2003 to 2014/2015. Values are calculated within the margins of the applied polynya mask (Fig. 1) and saturated at a level of 6 x 10^4 km^2 for a better discrimination of lower values.

During the freezing period (roughly October to June), fast ice forms along the coastlines of the Laptev Sea, which usually reaches its maximum areal extent by April. The approximate location of the fast-ice edge at the end of March is depicted in Fig. 9. For drifting sea ice, the fast-ice edge forms an advanced coast line with heavy ridging occurring along this edge during onshore wind events (Rigor and Colony, 1997). The combination of this fast-ice edge and off-shore components of the mean wind-patterns enable the formation of several flaw-lead polynyas across the Laptev Sea which can reach widths of up to 200 km (Bareiss and Görgen, 2005; Martin and Cavalieri, 1989; Ernsdorf et al., 2011; Adams et al., 2013).

When comparing previous studies dealing with ice production rates in the Laptev Sea (Dethleff et al., 1998; Winsor and Björk, 2000; Dmitrenko et al., 2009; Willmes et al., 2011; Tamura and Ohshima, 2011; Bauer et al., 2013; Iwamoto et al., 2014; Gutjahr et al., 2016), it gets clear that there are large differences depending on the applied methods and various different data-sets. In these studies, values for the accumulated ice production during an average winter season ('extended' winter-period from November to April) are ranging between 55 km^3 (Willmes et al., 2011) for an approach using microwave and thermal infrared remote sensing data in combination with atmospheric reanalysis data, and 258 km^3 (Dethleff et al., 1998), who used a simple relationship between wind direction/speed and polynya area. Estimated average values (September to May) from Tamura and Ohshima (2011) (152 km^3) and Iwamoto et al. (2014) (77 km^3) range in between. Although derived for different time periods and slightly varying reference areas, these large discrepancies highlight the relevance of applying improved and high-resolution approaches to quantify sea-ice production.

In order to give an overview on the long-term development of thin-ice areas (TIT $\leq$ 0.2 m) in the Laptev Sea, the daily POLA is presented in Fig. 10. It is evident that the largest areas of thin-ice appear on average in November and more recently also in December (compare Tab. 2). A tendency towards an increased duration of these polynya-events can be observed. In the winter-seasons 2008/2009 and 2009/2010, large POLA exceeding 50000 km^2 are also observed in January and another

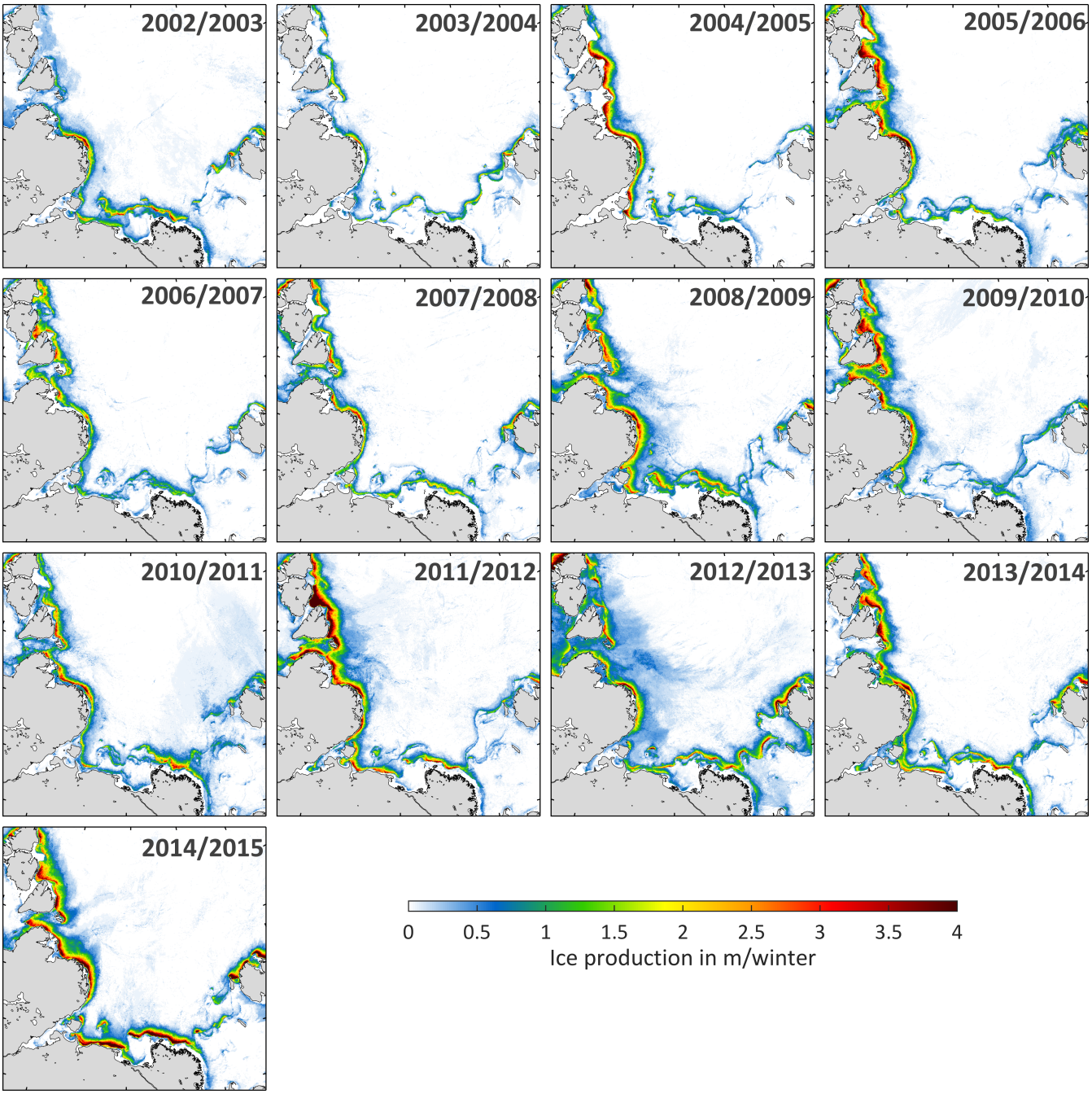

Figure 11. Overview of wintertime (November to March) accumulated ice production (m per winter) in the Laptev Sea region between 2002/2003 and 2014/2015.

major polynya event can be noted for mid-February 2015. A pronounced seasonal variation is visible for the winter seasons 2004/2005, 2005/2006 and from 2010/2011 onwards, while the other years show less polynya activity (more lengthy periods with a closed polynya; white color in Fig. 10) and overall smaller polynya extents in February and March.

Fig. 11 shows an annual comparison (2002/2003 to 2014/2015) of accumulated (November to March) ice production (in m per winter) for the Laptev Sea. The highest ice-production rates of sometimes more than 4 m per winter occur predominantly in proximity of the Taymyr Peninsula and Severnaya Zemlya (western Laptev Sea), as well as along the southern fast-ice edge (mainly coastwards of the regions with high ice production). However, ice production in the eastern Laptev Sea (west and north of the New Siberian Islands) shows a greater interannual variability. Furthermore, it is striking that the position of the fast-ice edge in Fig. 11 is highly variable over the 13-yr record (as in Sect. 4.1, Fig. 8 (a)). However, it has to be noted that certain bands of higher ice production, especially in the south-eastern Laptev Sea, reflect the wintertime evolution of fast ice (compare Selyuzhenok et al., 2015) and are hence primarily related to the early winter period from November to December. Another interesting observation can be made in the Vilkitsky Strait, which is located in the western Laptev Sea south of Severnaya Zemlya (Fig. 9). The distribution of thin-ice areas contributing significantly to the total sea-ice production in that area seems to shift westwards towards the Kara Sea in several years (2005/2006 to 2012/2013 and 2014/2015). In some cases, the shape of these areas resembles an arch-type/ice-bridge pattern/mechanism, a feature that is commonly appearing e.g. in Nares Strait between Ellesmere Island and Greenland (Williams et al., 2007).

Krumpen et al. (2013) discovered that most of the ice being incorporated in the Transpolar Drift originates from the western and central part of the Laptev Sea. Further, it was indicated that the contribution from polynyas, while being generally small, is limited to events in proximity of the Laptev Sea boundaries. As noted before, the north-western Laptev Sea shows by far the largest contribution to the total wintertime ice production in the Laptev Sea polynyas, which implies a potential significant influence on the interannual variability of the ice export during winter. In order to check this hypothesis, we compare annual accumulated IP values to independently derived ice-area export (IAE) values (both presented as anomalies and normalized with their standard deviation) in Fig. 12 for 2002/2003 to 2014/2015. IAE values are taken from the updated time series of Krumpen et al. (2013), where they were calculated as the integral of the product between the eastward and northward component of the ice drift velocity and ice concentration at the northern boundary (NB) and eastern boundary (EB) of the Laptev Sea, respectively. Likewise to a high agreement between polynya area and across-boundary ice export (Krumpen et al., 2013), there is also a significant correlation between calculated ice production and the areal ice export ($r = 0.69$ with $p = 0.009$).

The spatial overview of annual ice production (Fig. 11) is supplemented by the previously shown time series of the average wintertime POLA and accumulated IP per winter (Fig. 5 and Fig. 6, respectively). Both time series of POLA and IP in the Laptev Sea show an overall positive trend (significant with $p \leq 0.01$), which can for the most part be traced back to larger thin-ice areas during the freeze-up period in November and December (as decribed above; Fig. 10). This is underlined by Tab. 2 and 3, which both reveal largest average values of POLA / IP and most significant trends during that period of winter. The average ice production from November to March in the Laptev Sea is estimated with about 96 ± 33 km^3 (2002/2003 - 2014/2015), with a positive trend of 6.8 km^3 per year. Compared to other Arctic polynyas (compare Tab. 3), this corresponds to a share of about 5% of the total ice production in polynya regions.

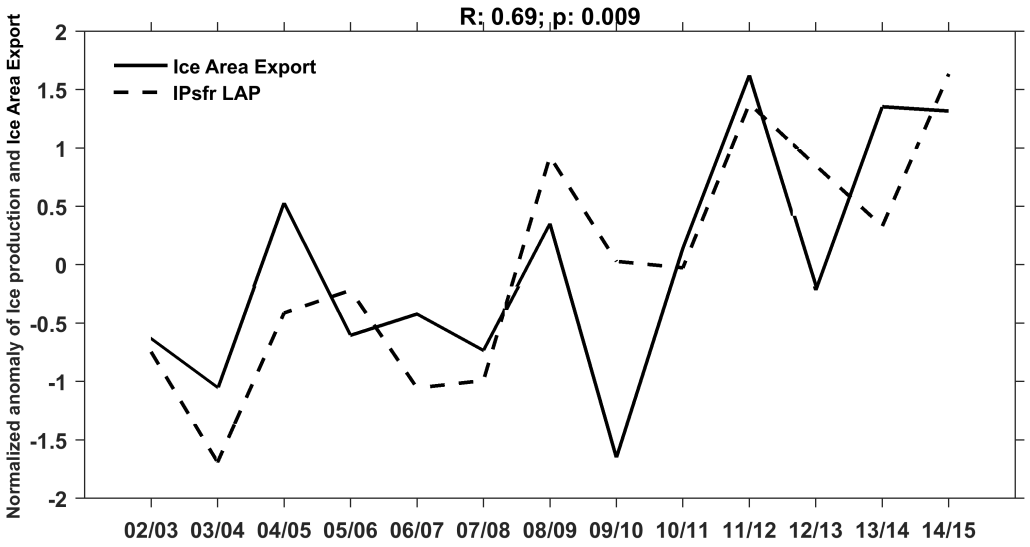

Figure 12. Normalized anomalies of accumulated wintertime ice production (IP of the present study; dashed line) and accumulated Ice Area Export (IAE; solid line) for winter seasons 2002/2003 to 2014/2015. IAE data is based on an updated time series by Krumpen et al. (2013).

As the relative strength of the Transpolar Drift is dependent on atmospheric dynamics, it has previously been linked to atmospheric indices like the Arctic Oscillation (AO) Index (Rigor and Wallace, 2004). For the period from 1982 to 2009, the study by Kwok et al. (2013) presented indicators for a net-strengthening of both the Transpolar Drift and the Beaufort Gyre as well as a general increase of the Arctic ice drift-speed~~. The latter is presumably connected~~ , which is presumably related to a decreasing fraction of thick multi-year (MY) ice~~and a more fragile, thus mobile,~~ . As mentioned before (Sect. 4.1), the latter is thought to be connected to an increased fragility and mobility of the Arctic sea-ice cover~~with potential~~ , which may have implications for polynya and lead dynamics not only in the eastern Arctic. According to Rigor et al. (2002), a positive winter AO promotes both an increased ice transport out of the Arctic Ocean through Fram Strait and an increased ice transport away from the Siberian coastal areas, thereby leaving open water and thin ice that foster new ice formation. Hence, positive trends in both POLA and IP not only fit well to the previously estimated positive trend in IP from Iwamoto et al. (2014) but also to the positive trend of 0.85 x 10^5 km^2 per decade in the Laptev Sea ice area flux (Krumpen et al., 2013). Other linkages and dependencies with the Arctic sea-ice extent in September (annual minimum), the timing of the freeze-onset and further connections to large-scale atmospheric circulation patterns are very likely and have been proposed by various previous studies (e.g. Alexandrov et al., 2000; Deser et al., 2000; Rigor et al., 2002; Willmes et al., 2011; Krumpen et al., 2013). Particularly a significant lengthening of the melt season in recent years and hence a later freeze-up in autumn already seems to imprint on the derived POLA (i.e. thin-ice area) and IP estimates in the early winter period (Markus et al., 2009; Parkinson, 2014; Stroeve et al., 2014). In that context, increasing atmosphere- and ocean-temperatures in autumn and winter have recently been reported by Boisvert and Stroeve (2015) that comprise the potential to alter/shift vertical temperature gradients with consequences for

the surface energy balance and ultimately IP. Further, a shortened fast-ice duration and enhanced variability of the fast-ice edge in early winter (Yu et al., 2014; Selyuzhenok et al., 2015) presumably influences the location of flaw leads and consequently high ice production / brine release. Frankly, all these (potential) interconnections are rather complex and would require more detailed investigations that go beyond the scope of the present study. In the context of other reported changes during the spring and summer period (Janout et al., 2016), it may emerge that the overall set-up for atmosphere-ice-ocean interactions in the Laptev Sea is gradually changing towards a new state.

5 Conclusions

In the present study we analyzed circumpolar polynya dynamics and ice production in the Arctic based on high-resolution MODIS thermal infrared imagery and atmospheric reanalysis from the ERA-Interim data set. Pan-Arctic and (quasi-) daily thin-ice thickness distributions were calculated using a 1D-energy balance model for the period from 2002/2003 to 2014/2015 (November to March). After applying a necessary and well-working gap-filling approach to compensate for cloud and data gaps, the thermodynamic ice production was derived by assuming that all heat loss at the ice surface contributes to the growth of sea ice. We presented results for 17 prominent polynya regions, whereby the a strong focus was set on the Laptev Sea region in the eastern Arctic. Despite existing limitations originating from the use of thermal infrared remote sensing data during winter, we think that this new data set of 13 consecutive winter seasons is a huge step forward for a spatially accurate characterization of Arctic polynya dynamics and the associated sea-ice budget related to winter-time sea-ice production. Our main findings and conclusions are the following:

(1) The use of high-resolution MODIS data enables the detection of thin ice much closer to the coast or fast-ice edges, mitigates land spill-over effects efficiently and generally increases the capability to resolve small scale (> 2km) thin-ice features such as narrow polynyas and leads, which therefore contribute to our ice production estimates. This represents an advantage compared to other (passive microwave) data sets.

(2) The average wintertime accumulated ice production in all 17 polynya regions is estimated with about $1811 \pm 293\ \mathrm{km}^3$. The largest contributions originate from the western proximity of Novaya Zemlya (20%), the Kara Sea region and the North Water polynya (both 15%) as well as scattered smaller polynyas in the (eastern) Canadian Arctic Archipelago (all combined around 12%). ~~Compared to the most recent study on ice production in Arctic polynyas by Iwamoto et al. (2014)~~By relying on predefined and fixed polynya masks, these IP estimates can include both thermodynamic ice growth within detected polynya margins (TIT ≤ 0.2 m) as well as ice production in open ocean / MIZ areas. However, our estimate on the average total ice production ~~is~~ exceeds that of Iwamoto et al. (2014) by about 52-54%~~larger, although~~. We note that differences in the regarded time frame, reference areas, sensor-specifics as well as a potential bias due to cloud cover and/or the exclusive assumption of clear-sky conditions certainly contribute to this discrepancy.

(3) Positive trends in ice production can be detected for several regions of the eastern Arctic (most significant in the Laptev Sea region with an increase of 6.8 km^3/yr and the North Water polynya, while other polynyas in the western Arctic show a more pronounced interannual variability. These regionally different trends could potentially originate from changes in the

overall sea-ice mobility (i.e. sea-ice drift), a temporal shift of the freeze onset in autumn (leading to larger thin-ice areas in November and December) or distinct large-scale atmospheric set-ups that promote an increased ice export and enhanced ice production in the Siberian shelf regions during winter.

(4) The Laptev Sea region was chosen as a special focus in our study as it is one of the core areas for ice production in the Arctic with a distinct connection to Transpolar Drift characteristics and showing a strong positive trend. Ice production in the Laptev Sea was mapped with enhanced spatial detail, which is especially valuable in this region with narrow and elongated flaw leads close to the fast-ice edge. Our results showed that polynyas in the Laptev Sea contribute with at least 5% to the total potential sea-ice production in Arctic polynyas. While the interannual variability in terms of location and extent seems to be rather high, the positive trends in both POLA and IP time series fit well to results and observations from other recently published studies in the Laptev Sea. A clear relation between increasing sea-ice area export (Krumpen et al., 2013) and positive trends in IP could be demonstrated, and future comparisons with recently derived volume-flux estimates in the Transpolar Drift (Krumpen et al., 2016) certainly promise further insights on the absolute contribution of polynyas to the volume ice export out of the Laptev Sea and adjacent seas.

(5) Compared to the MODIS-derived lead product by Willmes and Heinemann (2016), the SFR-algorithm used in the present study is not able to adequately reconstruct leads with a low spatial and temporal persistence. A thoughtful combination of both concepts is therefore a goal worth to achieve for future investigations on thin-ice regions in the polar regions using thermal infrared data from MODIS or other comparable satellite sensors, allowing for estimates of IP by leads also for the central Arctic ocean.

Author contributions. Andreas Preußer carried out the complete analysis and drafted the manuscript. Sascha Willmes and Stephan Paul supported the satellite data analysis and further processing. All co-authors contributed to the writing of the manuscript. The final draft of the manuscript was revised and approved by all of the authors.

Acknowledgements. The authors want to thank the National Snow and Ice Data Center (NSIDC) as well as the European Center for Medium-Range Weather Forecasts (ECMWF) for providing the MODIS Sea Ice product (ftp://n5eil01u.ecs.nsidc.org/SAN/) and the ERA-Interim atmospheric reanalysis data. The provision of the ice area export data set by Dr. Thomas Krumpen (Alfred Wegener Institute, Bremerhaven, Germany) as well as related discussions are highly acknowledged. Additional thanks to the three referees and the editor Dr. Dirk Notz, who helped to improve the manuscript with their highly valuable comments and suggestions during the review. This work was funded by the Federal Ministry of Education and Research (Bundesministerium für Bildung und Forschung - BMBF) under Grant 03G0833D.

References

ACIA: Arctic Climate Impact Assessment. ACIA Overview report., Cambridge University Press, 2005.

Ackerman, S., Frey, R., Strabala, K., Liu, Y., Gumley, L., Baum, B., and Menzel, P.: Discriminating clear-sky from cloud with MODIS algorithm theoretical basis document (MOD35) Version 6.1, Tech. rep., MODIS Cloud Mask Team, Cooperative Institute for Meteorological Satellite Studies, University of Wisconsin, 2010.

Adams, S., Willmes, S., Schroeder, D., Heinemann, G., Bauer, M., and Krumpen, T.: Improvement and sensitivity analysis of thermal thin-ice retrievals, IEEE Transactions on Geoscience and Remote Sensing, 51, 3306–3318, doi:10.1109/tgrs.2012.2219539, 2013.

Alexandrov, V. Y., Martin, T., Kolatschek, J., Eicken, H., Kreyscher, M., and Makshtas, A. P.: Sea ice circulation in the Laptev Sea and ice export to the Arctic Ocean: Results from satellite remote sensing and numerical modeling, Journal of Geophysical Research, 105, 17 143–17 159, 2000.

Barber, D. G. and Massom, R. A.: The Role of Sea Ice in Arctic and Antarctic Polynyas, in: Polynyas - Windows to the World, edited by Smith, W. O. and Barber, D. G., chap. The Role of Sea Ice in Arctic and Antarctic Polynyas, pp. 1–54, Elsevier Oceanography Series, doi:10.1016/s0422-9894(06)74001-6, 2007.

Bareiss, J. and Görgen, K.: Spatial and temporal variability of sea ice in the Laptev Sea: Analyses and review of satellite passive-microwave data and model results, 1979 to 2002, Global and Planetary Change, 48, 28–54, 2005.

Bauch, D., Hlemann, J. A., Dmitrenko, I. A., Janout, M. A., Nikulina, A., Kirillov, S. A., Krumpen, T., Kassens, H., and Timokhov, L.: Impact of Siberian coastal polynyas on shelf-derived Arctic Ocean halocline waters, J. Geophys. Res., 117, n/a–n/a, doi:10.1029/2011jc007282, http://dx.doi.org/10.1029/2011JC007282, 2012.

Bauer, M., Schröder, D., Heinemann, G., Willmes, S., and Ebner, L.: Quantifying polynya ice production in the Laptev Sea with the COSMO model, Polar Research, 32, doi:10.3402/polar.v32i0.20922, http://www.polarresearch.net/index.php/polar/article/view/20922, 2013.

Beitsch, A., Kaleschke, L., and Kern, S.: Investigating High-Resolution AMSR2 Sea Ice Concentrations during the February 2013 Fracture Event in the Beaufort Sea, Remote Sensing, 6, 3841–3856, doi:10.3390/rs6053841, http://dx.doi.org/10.3390/rs6053841, 2014.

Boisvert, L. N. and Stroeve, J. C.: The Arctic is becoming warmer and wetter as revealed by the Atmospheric Infrared Sounder, Geophysical Research Letters, 42, 4439–4446, doi:10.1002/2015GL063775, http://dx.doi.org/10.1002/2015GL063775, 2015GL063775, 2015.

Bromwich, D. H., Wilson, A. B., Bai, L.-S., Moore, G. W. K., and Bauer, P.: A comparison of the regional Arctic System Reanalysis and the global ERA-Interim Reanalysis for the Arctic, Quarterly Journal of the Royal Meteorological Society, 142, 644–658, doi:10.1002/qj.2527, http://dx.doi.org/10.1002/qj.2527, 2015.

Cohen, J., Screen, J. A., Furtado, J. C., Barlow, M., Whittleston, D., Coumou, D., Francis, J., Dethloff, K., Entekhabi, D., Overland, J., and Jones, J.: Recent Arctic amplification and extreme mid-latitude weather, Nature Geoscience, 7, 627–637, doi:10.1038/ngeo2234, http://dx.doi.org/10.1038/ngeo2234, 2014.

Dee, D. P., Uppala, S. M., Simmons, A. J., Berrisford, P., Poli, P., Kobayashi, S., Andrae, U., Balmaseda, M. A., Balsamo, G., Bauer, P., Bechtold, P., Beljaars, A. C. M., van de Berg, L., Bidlot, J., Bormann, N., Delsol, C., Dragani, R., Fuentes, M., Geer, A. J., Haimberger, L., Healy, S. B., Hersbach, H., Hólm, E. V., Isaksen, L., Kållberg, P., Köhler, M., Matricardi, M., McNally, A. P., Monge-Sanz, B. M., Morcrette, J.-J., Park, B.-K., Peubey, C., de Rosnay, P., Tavolato, C., Thépaut, J.-N., and Vitart, F.: The ERA-Interim reanalysis: configuration and performance of the data assimilation system, Quarterly Journal of the Royal Meteorological Society, 137, 553–597, doi:10.1002/qj.828, 2011.

Deser, C., Walsh, J. E., and Timlin, M. S.: Arctic sea ice variability in the context of recent atmospheric circulation trends, Journal of Climate, 13, 617–633, 2000.

Dethleff, D., Loewe, P., and Kleine, E.: The Laptev Sea flaw leaddetailed investigation on ice formation and export during 1991/1992 winter season, Cold Regions Science and Technology, 27, 225–243, 1998.

Dmitrenko, I. A., Kirillov, S. A., Tremblay, L. B., Bauch, D., and Willmes, S.: Sea-ice production over the Laptev Sea shelf inferred from historical summer-to-winter hydrographic observations of 1960s–1990s, Geophysical Research Letters, 36, 2009.

Drucker, R., Martin, S., and Moritz, R.: Observations of ice thickness and frazil ice in the St. Lawrence Island polynya from satellite imagery, upward looking sonar, and salinity/temperature moorings, J. Geophys. Res., 108, 3149, doi:10.1029/2001jc001213, 2003.

Ebner, L., Schröder, D., and Heinemann, G.: Impact of Laptev Sea flaw polynyas on the atmospheric boundary layer and ice production using idealized mesoscale simulations, Polar Research, 30 (7210), 16, doi:10.3402/polar.v30i0.7210, 2011.

Ernsdorf, T., Schrder, D., Adams, S., Heinemann, G., Timmermann, R., and Danilov, S.: Impact of atmospheric forcing data on simulations of the Laptev Sea polynya dynamics using the sea-ice ocean model FESOM, J. Geophys. Res., 116, doi:10.1029/2010jc006725, http://dx.doi.org/10.1029/2010JC006725, 2011.

Gutjahr, O., Heinemann, G., Preußer, A., Willmes, S., and Drüe, C.: Sensitivity of ice production estimates in Laptev Sea polynyas to the parameterization of subgrid-scale sea-ice inhomogeneities in COSMO-CLM, The Cryosphere Discussions, 2016, 1–34, doi:10.5194/tc-2016-83, http://www.the-cryosphere-discuss.net/tc-2016-83/, 2016.

Haid, V., Timmermann, R., Ebner, L., and Heinemann, G.: Atmospheric forcing of coastal polynyas in the south-western Weddell Sea, Antarctic Science, 27, 388–402, doi:10.1017/s0954102014000893, http://dx.doi.org/10.1017/S0954102014000893, 2015.

Hall, D., Key, J., Casey, K., Riggs, G., and Cavalieri, D.: Sea ice surface temperature product from MODIS, Geoscience and Remote Sensing, IEEE Transactions on, 42, 1076 – 1087, doi:10.1109/tgrs.2004.825587, 2004.

Hannah, C. G., Dupont, F., and Dunphy, M.: Polynyas and tidal currents in the Canadian Arctic Archipelago, Arctic, pp. 83–95, 2009.

Heinemann, G. and Rose, L.: Surface energy balance, parameterizations of boundary-layer heights and the application of resistance laws near an Antarctic Ice Shelf front, Boundary-Layer Meteorology, 51, 123–158, doi:10.1007/bf00120464, http://dx.doi.org/10.1007/BF00120464, 1990.

Hirano, D., Fukamachi, Y., Watanabe, E., Ohshima, K. I., Iwamoto, K., Mahoney, A. R., Eicken, H., Simizu, D., and Tamura, T.: A wind-driven, hybrid latent and sensible heat coastal polynya off Barrow, Alaska, Journal of Geophysical Research: Oceans, doi:10.1002/2015JC011318, 2016.

Iwamoto, K., Ohshima, K. I., and Tamura, T.: Improved mapping of sea ice production in the Arctic Ocean using AMSR-E thin ice thickness algorithm, Journal of Geophysical Research: Oceans, 119, 3574–3594, doi:10.1002/2013jc009749, http://onlinelibrary.wiley.com/doi/10.1002/2013JC009749/abstract, 2014.

Jakobsson, M., Mayer, L., Coakley, B., Dowdeswell, J. A., Forbes, S., Fridman, B., Hodnesdal, H., Noormets, R., Pedersen, R., Rebesco, M., Schenke, H. W., Zarayskaya, Y., Accettella, D., Armstrong, A., Anderson, R. M., Bienhoff, P., Camerlenghi, A., Church, I., Edwards, M., Gardner, J. V., Hall, J. K., Hell, B., Hestvik, O., Kristoffersen, Y., Marcussen, C., Mohammad, R., Mosher, D., Nghiem, S. V., Pedrosa, M. T., Travaglini, P. G., and Weatherall, P.: The international bathymetric chart of the Arctic Ocean (IBCAO) version 3.0, Geophysical Research Letters, 39, doi:10.1029/2012gl052219, 2012.

Janout, M., Hölemann, J., Juhls, B., Krumpen, T., Rabe, B., Bauch, D., Wegner, C., Kassens, H., and Timokhov, L.: Episodic warming of near-bottom waters under the Arctic sea ice on the central Laptev Sea shelf, Geophysical Research Letters, 43, 264–272, doi:10.1002/2015GL066565, http://dx.doi.org/10.1002/2015GL066565, 2015GL066565, 2016.

Kern, S.: Polynya area in the Kara Sea, Arctic, obtained with microwave radiometry for 1979–2003, Geoscience and Remote Sensing Letters, IEEE, 5, 171–175, 2008.

König-Langlo, G. and Augstein, E.: Parameterization of the downward long-wave radiation at the Earth's surface in polar regions, Meteorologische Zeitschrift, N.F.3, 343–347, hdl:10013/epic.12338, 1994.

Krumpen, T., Janout, M., Hodges, K., Gerdes, R., Girard-Ardhuin, F., Hölemann, J., and Willmes, S.: Variability and trends in Laptev Sea ice outflow between 1992–2011, The Cryosphere, 7, 1–15, 2013.

Krumpen, T., Gerdes, R., Haas, C., Hendricks, S., Herber, A., Selyuzhenok, V., Smedsrud, L., and Spreen, G.: Recent summer sea ice thickness surveys in Fram Strait and associated ice volume fluxes, The Cryosphere, 10, 523–534, doi:10.5194/tc-10-523-2016, http://www.the-cryosphere.net/10/523/2016/, 2016.

Kwok, R., Spreen, G., and Pang, S.: Arctic sea ice circulation and drift speed: Decadal trends and ocean currents, Journal of Geophysical Research: Oceans, 118, 2408–2425, 2013.

Laxon, S. W., Giles, K. A., Ridout, A. L., Wingham, D. J., Willatt, R., Cullen, R., Kwok, R., Schweiger, A., Zhang, J., Haas, C., Hendricks, S., Krishfield, R., Kurtz, N., Farrell, S., and Davidson, M.: CryoSat-2 estimates of Arctic sea ice thickness and volume, Geophysical Research Letters, 40, 732–737, doi:10.1002/grl.50193, http://dx.doi.org/10.1002/grl.50193, 2013.

Liu, Y. and Key, J. R.: Less winter cloud aids summer 2013 Arctic sea ice return from 2012 minimum, Environmental Research Letters, 9, 044 002, doi:10.1088/1748-9326/9/4/044002, http://dx.doi.org/10.1088/1748-9326/9/4/044002, 2014.

Mahoney, A. R., Eicken, H., Gaylord, A. G., and Gens, R.: Landfast sea ice extent in the Chukchi and Beaufort Seas: The annual cycle and decadal variability, Cold Regions Science and Technology, 103, 41–56, doi:10.1016/j.coldregions.2014.03.003, http://dx.doi.org/10.1016/j.coldregions.2014.03.003, 2014.

Markus, T., Stroeve, J. C., and Miller, J.: Recent changes in Arctic sea ice melt onset, freezeup, and melt season length, J. Geophys. Res., 114, doi:10.1029/2009jc005436, http://dx.doi.org/10.1029/2009JC005436, 2009.

Martin, S.: Frazil ice in rivers and oceans, Annual Review of Fluid Mechanics, 13, 379–397, doi:10.1146/annurev.fl.13.010181.002115, 1981.

Martin, S. and Cavalieri, D. J.: Contributions of the Siberian shelf polynyas to the Arctic Ocean intermediate and deep water, Journal of Geophysical Research: Oceans, 94, 12 725–12 738, 1989.

Melling, H., Haas, C., and Brossier, E.: Invisible polynyas: Modulation of fast ice thickness by ocean heat flux on the Canadian polar shelf, Journal of Geophysical Research, Oceans, 120, 777–795, doi:10.1002/2014jc010404, http://dx.doi.org/10.1002/2014JC010404, 2015.

Moore, G. W. K., Bromwich, D. H., Wilson, A. B., Renfrew, I., and Bai, L.: Arctic System Reanalysis improvements in topographically forced winds near Greenland, Quarterly Journal of the Royal Meteorological Society, 142, 2033–2045, doi:10.1002/qj.2798, http://dx.doi.org/10.1002/qj.2798, 2016.

Morales-Maqueda, M., Willmott, A., and Biggs, N.: Polynya dynamics: A review of observations and modeling, Reviews of Geophysics, 42, 1–37, doi:10.1029/2002rg000116, 2004.

Parkinson, C. L.: Spatially mapped reductions in the length of the Arctic sea ice season, Geophys. Res. Lett., 41, 4316–4322, doi:10.1002/2014gl060434, http://dx.doi.org/10.1002/2014GL060434, 2014.

Parkinson, C. L. and Comiso, J. C.: On the 2012 record low Arctic sea ice cover: Combined impact of preconditioning and an August storm, Geophysical Research Letters, 40, 1356–1361, 2013.

Paul, S., Willmes, S., Gutjahr, O., Preußer, A., and Heinemann, G.: Spatial Feature Reconstruction of Cloud-Covered Areas in Daily MODIS Composites, Remote Sensing, 7, 5042–5056, doi:10.3390/rs70505042, 2015a.

Paul, S., Willmes, S., and Heinemann, G.: Long-term coastal-polynya dynamics in the Southern Weddell Sea from MODIS thermal-infrared imagery, The Cryosphere, 9, 2027–2041, doi:10.5194/tc-9-2027-2015, 2015b.

Preußer, A., Heinemann, G., Willmes, S., and Paul, S.: Multi-Decadal Variability of Polynya Characteristics and Ice Production in the North Water Polynya by Means of Passive Microwave and Thermal Infrared Satellite Imagery, Remote Sensing, 7, 15 844–15 867, 2015a.

Preußer, A., Willmes, S., Heinemann, G., and Paul, S.: Thin-ice dynamics and ice production in the Storfjorden polynya for winter seasons 2002/2003-2013/2014 using MODIS thermal infrared imagery, The Cryosphere, 9, 1063–1073, doi:10.5194/tc-9-1063-2015, http://www.the-cryosphere.net/9/1063/2015/, 2015b.

Riggs, G., Hall, D., and Salomonson, V.: MODIS Sea Ice Products User Guide to Collection 5, National Snow and Ice Data Center, University of Colorado, Boulder, CO 80309-0449 USA, http://nsidc.org/data/docs/daac/modis_v5/dorothy_ice_doc.pdf, 2006.

Rigor, I. and Colony, R.: Sea-ice production and transport of pollutants in the Laptev Sea, 1979–1993, Science of the Total Environment, 202, 89–110, 1997.

Rigor, I. G. and Wallace, J. M.: Variations in the age of Arctic sea-ice and summer sea-ice extent, Geophysical Research Letters, 31, 2004.

Rigor, I. G., Wallace, J. M., and Colony, R. L.: Response of sea ice to the Arctic Oscillation, Journal of Climate, 15, 2648–2663, 2002.

Schweiger, A., Lindsay, R., Zhang, J., Steele, M., Stern, H., and Kwok, R.: Uncertainty in modeled Arctic sea ice volume, Journal of Geophysical Research, 116, doi:10.1029/2011jc007084, http://dx.doi.org/10.1029/2011JC007084, 2011.

Selyuzhenok, V., Krumpen, T., Mahoney, A., Janout, M., and Gerdes, R.: Seasonal and interannual variability of fast ice extent in the southeastern Laptev Sea between 1999 and 2013, Journal of Geophysical Research: Oceans, lera, 2015.

Smith, S. D., Muench, R. D., and Pease, C. H.: Polynyas and leads: An overview of physical processes and environment, Journal of Geophysical Research, 95, 9461–9479, doi:10.1029/jc095ic06p09461, 1990.

Spreen, G., Kaleschke, L., and Heygster, G.: Sea ice remote sensing using AMSR-E 89 GHz channels, Journal of Geophysical Research, 113, doi:10.1029/2005JC003384, 2008.

Steffen, K.: Warm water cells in the North Water, northern Baffin Bay during winter, Journal of Geophysical Research: Oceans, 90, 9129–9136, doi:10.1029/JC090iC05p09129, 1985.

Stroeve, J., Markus, T., Boisvert, L., Miller, J., and Barrett, A.: Changes in Arctic melt season and implications for sea ice loss, Geophysical Research Letters, 41, 1216–1225, 2014.

Tamura, T. and Ohshima, K. I.: Mapping of sea ice production in the Arctic coastal polynyas, J. Geophys. Res., 116, C07 030, doi:10.1029/2010jc006586, 2011.

Tamura, T., Ohshima, K. I., Markus, T., Cavalieri, D. J., Nihashi, S., and Hirasawa, N.: Estimation of Thin Ice Thickness and Detection of Fast Ice from SSM/I Data in the Antarctic Ocean, J. Atmos. Oceanic Technol., 24, 1757–1772, doi:10.1175/jtech2113.1, 2007.

Tamura, T., Ohshima, K. I., and Nihashi, S.: Mapping of sea ice production for Antarctic coastal polynyas, Geophys. Res. Lett., 35, L07 606, doi:10.1029/2007gl032903, 2008.

Timco, G. and Frederking, R.: A review of sea ice density, Cold Regions Science and Technology, 24, 1–6, doi:10.1016/0165-232X(95)00007-X, 1996.

Timmermans, M.-L.: The impact of stored solar heat on Arctic sea ice growth, Geophysical Research Letters, 42, 6399–6406, 2015.

Williams, W. J., Carmack, E. C., and Ingram, R. G.: Physical Oceanography of Polynyas, in: Polynyas - Windows to the World, edited by Smith, W. O. and Barber, D. G., chap. Physical Oceanography of Polynyas, pp. 55–86, Elsevier, 2007.

Willmes, S. and Heinemann, G.: Sea-Ice Wintertime Lead Frequencies and Regional Characteristics in the Arctic, 2003–2015, Remote Sensing, 8, 4, 2016.

Willmes, S., Krumpen, T., Adams, S., Rabenstein, L., Haas, C., Hoelemann, J., Hendricks, S., and Heinemann, G.: Cross-validation of polynya monitoring methods from multisensor satellite and airborne data: a case study for the Laptev Sea, Canadian Journal of Remote Sensing, 36, S196–S210, doi:10.5589/m10-012, 2010.

Willmes, S., Adams, S., Schröder, D., and Heinemann, G.: Spatio-temporal variability of polynya dynamics and ice production in the Laptev Sea between the winters of 1979/80 and 2007/08, Polar Research, 30 (5971), 16, doi:10.3402/polar.v30i0.5971, 2011.

Winsor, P. and Björk, G.: Polynya activity in the Arctic Ocean from 1958 to 1997, Journal of Geophysical Research, 105, 8789–8803, 2000.

Yao, T. and Tang, C.: The formation and maintenance of the North Water polynya, Atmosphere-Ocean, 41, 187–201, 2003.

Yu, Y. and Lindsay, R.: Comparison of thin ice thickness distributions derived from RADARSAT Geophysical Processor System and advanced very high resolution radiometer data sets, J. Geophys. Res., 108, 3387, doi:10.1029/2002jc001319, 2003.

Yu, Y. and Rothrock, D. A.: Thin ice thickness from satellite thermal imagery, J. Geophys. Res., 101, 25 753–25 766, doi:10.1029/96jc02242, 1996.

Yu, Y., Stern, H., Fowler, C., Fetterer, F., and Maslanik, J.: Interannual Variability of Arctic Landfast Ice between 1976 and 2007, Journal of Climate, 27, 227–243, doi:10.1175/jcli-d-13-00178.1, http://dx.doi.org/10.1175/JCLI-D-13-00178.1, 2014.